INVESTIGATION OF THE EFFECTS OF A NOVEL DEFROST METHOD ON COOLING SYSTEM PERFORMANCE

2021
Ph. D. THESIS
MECHANICAL ENGINEERING

MAHADE OMRAN ALI ABDULLA

Prof. Dr. Emrah DENİZ

INVESTIGATION OF THE EFFECTS OF A NOVEL DEFROST METHOD ON COOLING SYSTEM PERFORMANCE

Mahade Omran Ali ABDULLA

T.C.
Karabuk University
Institute of Graduate Programs
Department of Mechanical Engineering
Prepared as
Ph. D. Thesis

Prof. Dr. Emrah DENİZ

KARABUK
Jun 2021

I certify that in my opinion the thesis submitted by Mahade Omran Ali ABDULLA titled “INVESTIGATION OF THE EFFECTS OF A NOVEL DEFROST METHOD ON COOLING SYSTEM PERFORMANCE” is fully adequate in scope and quality as a thesis for the degree of Ph. D.

Prof. Dr. Emrah DENİZ .....
Thesis Advisor, Department of Mechanical Engineering

This thesis is accepted by the examining committee with a unanimous vote in the Department of Mechanical Engineering as a Ph. D. thesis. Jun 28, 2021

Examining Committee Members (Institutions)	Signature
Chairman : Prof. Dr. Ahmet Korhan BİNARK (İZÜ)	Online
Member : Prof. Dr. Emrah DENİZ (KBÜ)	.....
Member : Doç. Dr. Ali Etem GÜREL (DÜ)	Online
Member : Doç. Dr. Mustafa KARAGÖZ (KBÜ)	.....
Member : Doç. Dr. Bahadır ACAR (KBÜ)	.....

The degree of Ph. D. of Science by the thesis submitted is approved by the Administrative Board of the Institute of Graduate Programs, Karabuk University.

Prof. Dr. Hasan SOLMAZ..... .....
Director of the Institute of Graduate Programs

"I declare that all the information within this thesis has been gathered and presented in accordance with academic regulations and ethical principles and I have according to the requirements of these regulations and principles cited all those which do not originate in this work as well."

Mahade Omran Ali ABDULLA

ABSTRACT

Ph. D. Thesis

INVESTIGATION OF THE EFFECTS OF A NOVEL DEFROST METHOD ON COOLING SYSTEM PERFORMANCE

Mahade Omran Ali ABDULLA

Karabük University
Institute of Graduate Programs
The Department of Mechanical Engineering

Thesis Advisor:
Prof. Dr. Emrah DENİZ
Jun 2021, 109 pages

In refrigeration systems, frost accumulation occurs on the evaporators under operating conditions below the freezing point of water and the dew point of the air. Depending on the increase in the amount of accumulated frost, the performance of the system decreases, and energy consumption increases. Therefore, it is necessary to start the defrosting process from time to time, which causes extra energy consumption. Traditional defrosting methods need time and energy to complete, which causes temperature fluctuations and decreases refrigeration efficiency in storage rooms during the defrost process. This study aims to reduce the energy required for defrosting and increase the cooling performance by using a liquid refrigerant for defrosting. For this purpose, two evaporators and a four-way valve were used in the system, thus reducing temperature fluctuations during the defrosting process. When the room is cooled with one of the evaporators, the other one has used for sub-cooling the refrigerant before entering the cooler evaporator. With the sub-cooling process, the second evaporator is defrosted. When the cooler evaporator needs to be defrosted, the second evaporator will be cooler. When the cycle is reversed using the four-way valve, the first evaporator will be defrosted and sub-cooler the liquid refrigerant. For this purpose, a cold room

operating with a vapor-compression refrigeration cycle was built and experimentally tested. Environmental, economic, exergy, and energy analyses (4E analysis) on both systems were conducted and these results were then compared. The findings of this study showed that the new method can perform the defrosting process using energy dissipated from the sub-cooling refrigerant without the use of any external source of power and thus enhance the refrigeration efficiency by 12%. Furthermore, this system does not resemble traditional defrost systems such that it does not interrupt the cooling process during the defrosting process as is the case with traditional systems.

Keywords: Defrost Efficiency, Cold Storage Room, 4E Analysis, Defrosting Method, Sub-Cooling.

Science Code: 91408

ÖZET

Doktora Tezi

TASARLANAN YENİ BİR DEFROST YÖNTEMİNİN SOĞUTMA SİSTEM PERFORMANSI ÜZERİNDEKİ ETKİLERİNİN İNCELENMESİ

Mahade Omran Ali ABDULLA

Karabük Üniversitesi
Lisansüstü Eğitim Enstitüsü
Makina Mühendisliği Anabilim Dalı

Tez Danışmanı:
Prof. Dr. Emrah DENİZ
Haziran 2021, 109 sayfa

Soğutma sistemlerinde, suyun donma noktası ve havanın yoğuşma noktası sıcaklıklarının altındaki çalışma koşullarında evaporatörlerin üzerinde buz birikmesi meydana gelir ve biriken buzun miktarındaki artışa bağlı olarak sistemin performansı düşer ve enerji tüketimi artar. Bu nedenle, ilave enerji tüketimine neden olan defrost işleminin zaman zaman başlatılması gerekir. Geleneksel buz çözme yöntemlerinin tamamlanması için zamana ve enerjiye ihtiyaç vardır, bu da buz çözme işlemi sırasında sıcaklık dalgalanmasına neden olur ve depolama odasındaki soğutma verimliliğini azaltır. Bu çalışmada, defrost işlemi için sıvı soğutucu akışkan kullanılarak, defrost işlemi için gerekli enerjinin azaltılması ve soğutma performansının arttırılması hedeflenmiştir. Bu amaçla, sistemde iki evaporatör ve bir dört yollu valf kullanılmıştır ve böylelikle defrost işlemi esnasında sıcaklık dalgalanmasının da azaltılması sağlanmıştır. Evaporatörlerden biri ile oda soğutulduğunda diğeri soğutu akışkanı evaporatöre girmeden önce aşırı soğutmak için kullanılmıştır. Aşırı soğutma işlemi ile, ikinci evaporatörün buzunun çözülmesi (defrost) sağlanır. Soğutucu evaporatörün

buzunun çözülmesi gerektiğinde, ikinci evaporatör daha soğuk olacaktır. Döngü, dört yollu valf tarafından tersine çevrildiğinde, ilk evaporatör, defrost edilecek ve aşırı soğutucu olacaktır. Bu amaçla, buhar sıkıştırmalı soğutma çevrimi ile çalışan bir soğuk oda inşa edilmiş ve deneysel olarak test edilmiştir. Her iki sistem için çevresel, ekonomik, ekserji ve enerji analizleri (4E analizi) yapılmış ve bu sonuçlar karşılaştırılmıştır. Bu çalışmadan elde edilen bulgular, yeni yöntemin, herhangi bir harici güç kaynağı kullanmadan aşırı soğutulmuş akışkandan yayılan enerjiyi kullanarak defrost işlemini gerçekleştirebildiğini ve böylece soğutma verimliliğini %12 artırdığını göstermiştir. Ayrıca, bu sistem, geleneksel sistemlerde olduğu gibi defrost işlemi esnasında soğutma işlemini kesintiye uğratmadığı için geleneksel defrost sistemlerine benzememektedir.

Anahtar Kelimeler : Defrost Verimliliği, Soğuk Hava Deposu, 4E Analizi, Defrost Metodu, Aşırı Soğutma.

Bilim Kodu: 91408

ACKNOWLEDGMENT

First of all, I would like to thank my supervisor Prof. Dr. Emrah DENIZ for his supervision, support, and tutelage during my Ph.D. degree. My gratitude extends to the higher institute of refrigeration and air conditioning in Sokna and the Libyan Ministry of Education for the funding opportunity to undertake my studies at the Department of mechanical engineering, Karabük University in Turkey. I also thank Doç. Dr. Ali Etem GÜREL, Dr. Öğr. Üyesi Mustafa KARAGÖZ, for their mentorship. I would like to thank my friends, lab mates, colleagues, and research team Nuri TUNÇ, Muhammet Ufuk UÇAR, and Gürşah GÜRÜF for a cherished time spent together in the lab, and social settings. My appreciation also goes out to my family and friends for their encouragement and support all through my studies.

CONTENTS

Page

Page

Page

LIST OF FIGURES

Page

Page

LIST OF TABLES

Page

SYMBOLS AND ABBREVIATIONS

A	surface area	(m^2)
COP	coefficient of performance	
V	Volume	(m^3)
$\dot{Q}$	Heat transfer rate	(W)
$\dot{P}$	Power	(W)
P	Pressure	(bar)
S	Specific entropy	(kJ kg^{-1} K^{-1})
T	Temperature	(°C)
T	Time	(s)
I	Current	(A)
H	Specific enthalpy	(kJ kg^{-1})
Sc	Subcooling	(K)
Sh	Superheat	(K)
$\dot{W}$	Work	(W)
$\dot{E}$	Exergy rate	(W)
$\dot{m}$	mass flow rate	(g s^{-1})
L_p	low pressure	(bar)
H_p	high pressure	(bar)
f_i	heat of fusion	(kJ kg^{-1})
I	Annual interest rate	(%)
P	capital cost	($)
S	salvage value	($)

Z_{CO2}	environmental cost	($)

GREEK LETTERS

η	efficiency	(%)
ε	Effectiveness	(%)
ϕ_{CO_2}	CO_2 emissions	kg $year^{-1}$
Ψ_{CO_2}	CO_2 emissions	$kgCO_2$ kWh^{-1}

SUBSCRIPTS

a	ambient
Con	Condenser
Comp	Compressor
Def	Defrost
El	electrical
Hex	heat exchanger
In	Inlet
Is	Isentropic
Mec	mechanical
R	Refrigerant
O	dead state
Out	Outlet
ASV	annual salvage value
SFF	sinking fund factor
CRF	capital recovery factor
AEC	annual electric cost
FAC	fixed annual cost
APC	annual power consumption
AC	annual cost
CPC	cost of 1 kW of cooling

PART 1

INTRODUCTION

1.1. EARLY REFRIGERATION SYSTEMS

The refrigeration systems in the mid to the late nineties of the last century were not common due to their large size, inefficiency, and high costs. Also, they were needed full-time attention from an experienced operator. Nevertheless, the 20th century witnessed high and rapid development and growth in this industry. Currently, this growth and development are continued and include entering new technologies including electronic control systems and more effective elements such as coils and compressors to simplify the development of improved and more effective refrigeration systems. The mechanical design function of the refrigeration systems classifies them into five categories as follow [1].

- Domestic
- Commercial
- Industrial
- Marine and transport
- Air-conditioning

The domestic refrigeration systems comprise home freezers and fridges and represent a significant part of the refrigeration systems industry. The commercial refrigeration systems include vending machines and refrigerated cabinets used in supermarkets, restaurants, and grocery stores. The industrial refrigeration systems include large refrigerated systems found in many industrial facilities such as food processing places, ice cream factories, refrigerated warehouses, and dairies. The marine and transpiration refrigeration systems include systems on sea vessel containers, and truck and rail

refrigerated compartments whereas the air conditioning systems are popular in buses, large buildings, and cars to preserve the air conditioning.

Currently, societies are highly dependent on refrigeration industries by systems used in many types of applications. The air forced chillers are used to quickly freeze products including vegetables and fruits. Later, the products are stored in refrigerated warehouses at temperatures of −20°C. Then, the refrigerated products are distributed by using transport refrigeration systems into various places such as restaurants, supermarkets, groceries, and hotels. The groceries store the frozen and fresh products in a refrigerated display cabinet at temperatures of 4°C and −20°C respectively. In the end, the journey of products is finished from the harvest to be stored in domestic fridges and freezers. Another type of refrigeration system is air conditioning which is also used in trucks, trains, buses, and cars. Refrigeration systems are varied and different due to their use and applications and therefore, our study will focus on Cooling Room Refrigeration Systems and on enhancing the defrosting method. Nevertheless, since all the refrigeration systems have the same basic components and design layout, Cold Room Refrigeration System Defrost Method or transfer to other refrigeration systems may well be adopted.

1.1.1. Cold Storage Rooms

This method is widely used for bulk treatment of perishables between the manufacturing and marketing processes. It is considered one of the methods to store the perishables products freshly and wholesomely for long periods by adjusting the temperature and humidity inside the cold storage room. Maintaining low temperature adequately is considered an important issue otherwise, this will lead to product damage. Also, relative humidity in the cold rooms should be maintained as high as 80-90% for most of the perishables below or higher which harms the quality of the products. Most of the agricultural products are characterized by limited age after the harvest if they are preserved in normal harvesting temperature. The postharvest cooling quickly removes the field heat which allows a longer storage period. The advantages of suitable postharvest cooling can be summarized as follows [2]:

- Decrease the activity of the respiratory from deterioration by enzymes.
- Decease the wilting and internal loss of waters.
- Prevent or slow the decay growth produces the microorganisms.
- Decrease the production of natural ripening agents (ethylene).

Postharvest cooling preserves the quality of products and provides flexibility in marketing by allowing farmers to sell their products at all suitable times. The existence of cooling facilities and storing rooms makes it not necessary to market the products after the harvesting immediately. This provides advantages to farmers who aim to sell their products to hotels, groceries, restaurants, or small farmers who want to collect more trucks for consignment. Postharvest cooling is considered an important matter to transport high-quality products to the customers or selling points. It is possible to combine the cold storage rooms with storage in a specific environment by adding sulfur dioxide, carbon dioxide, etc. according to the nature of products to be preserved. In recent years, cold storage rooms were noticeably developed which led to enhance the preservation of organoleptic qualities, decrease spoilage and extend the life span. These developments resulted from the mutual job of physiologists to determine the vegetables and fruits requirements and by specialists of refrigeration to design and operate the cooling systems accordingly.

These advances have resulted from joint action by physiologists to define the requirements of fruit and vegetables, and by refrigerating specialists to design and operate refrigerating systems [1].

1.1.2. Refrigeration System in the Cooling Room

The cooling storage room diagram is shown in Figure 1.1 with a description of each of its parts. The heart of cooling systems is the compressor. The refrigerant is compressed by the compressor in the gaseous status, increases the temperature and pressure, in addition, to push it into the condenser. The condenser is a heat exchanger that operates to cool the gas and change it to liquid. When the steam is condensed into the liquid, it must pass a portion of the internal energy (condensation temperature) to the environment. The fan feds the heat. The pressure is highly dropped when the liquid

refrigerant passes through the expansion device (expansion valve). The refrigerant enters the evaporator as a liquid with low pressure; the refrigerant starts boiling up and evaporates, the evaporation arises a cooling impact in the evaporator. Then, the refrigerant leaves the evaporator as low pressure warm saturated gas. This circulation is closed and repeated continuously.

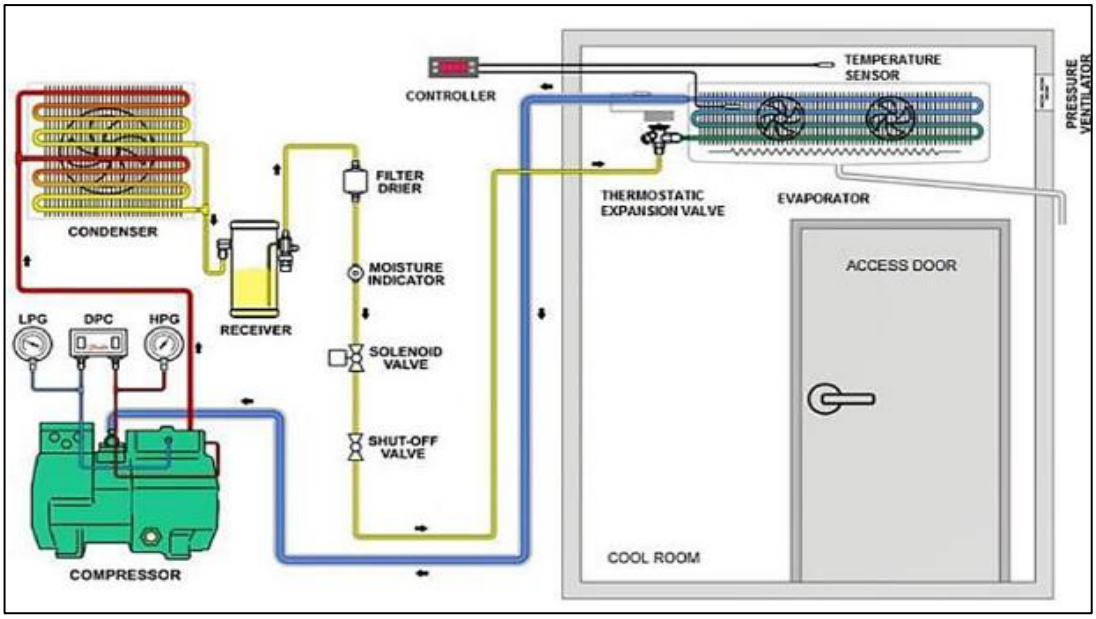

Figure 1.1. Cold storage refrigeration system piping diagram [3].

1.1.3. Frosting and Defrosting

The frosting is a desirable and famous phenomenon on evaporator coils in heat pumps and refrigeration systems. The frosting phenomenon occurs when the surface temperate of evaporator fins is lower than zero degrees and humid air passes over it. The frosting decreases the performance and capacity of the heat exchanger. The cycle of defrosting must be done periodically to maintain the capacity and performance of the evaporator.

1.2. RESEARCH PROBLEM AND JUSTIFICATION

Global warming is considered one of the most challenges and threats which faced the human being in the 21st century. The burning of fossil fuels is the main reason for to

increase in the amount of CO_2 in the atmosphere where CO_2 increased by about 34% from 1950 [3]. Consequently, industry by its various sectors is the main reason for this situation. Many efforts and initiatives were performed to address the climate change problem. For instance, the EU aimed to decrease the emissions of GHG by 20%, enhance energy efficiency by 20%, increase the use of clean and renewable energy by 20% in 2020 [4].

The demand for thermal energy is estimated to be 50% of the total energy demand in the world [3]. Efforts were already spent on renewable energy which does not serve the demands on thermal energy. Interest in renewable heating and cooling resources is the most important element in the work plan against climate change [5]. The refrigeration systems that operate in saturated air temperature less than the freezing point will at the end face frost accumulation on the evaporator fins and coils. The frost operates as a thermal insulator between the heat to be transferred from the space and the evaporator fins, resulting in a decrease in evaporator efficiency. The existence of a frosted medium increases the resistance of both the hydraulic and thermal in the airside of the evaporator. Both of these impacts reduce the capacity of refrigeration and increase compressor run-time that causes more energy consumption to achieve the required cooling effect. Therefore, the defrosting process has an important effect to raise the refrigeration system's efficiency.

1.2.1. Temperature Fluctuations

One of the most important factors which affect the quality of food is the food storage temperature. Typically, temperature fluctuations occur in the cold store during the defrosting process above the optimal temperature range. Increase the temperature in the cold store leads to encouraging circumstances to form the microorganism. Reduce the temperature to lower than the specified degree leads to food degradation. The temperature fluctuations can cause the degradation of food [6]. The heat loss from the defrosting device during the defrosting process can cause significant temperature fluctuation.

1.2.2. Social Concerns on Energy

The cold storages and supermarkets are the most energy consumption buildings, particularly in hot countries. The commercial refrigeration system energy which used in the USA [7]. A high amount of energy is used to preserve the frozen and chilled foods in both storage refrigerators and product display cases. The size of supermarkets is varied from one country to another. For example, in Europe, the size of stores ranges from around 500 m^2 to 3000 m^2 or a little larger. In Canada and the USA, stores are generally larger and range from around 1000 m^2 to 10000 m^2 [8]. The capacity of the plant ranges from 30 to 60 kW to small markets and reaches over 3060 kW in larger stores. Likewise, the annual use of energy ranges from 100000 kWh/y in small stores to more than 1.5 million kWh/y in larger stores [9]. A field study was conducted in Southern California about the electric energy consumption in supermarkets. the study showed that the refrigeration systems were the largest element that consumes energy in the supermarket it reaches half or more of the store totals. 53% of electric energy consumption was in refrigeration systems, 27% in lighting the store, 9% used in HVAC systems, and 11% were in other usages [8].

1.3. AIMS AND OBJECTIVES

Our study aims to develop improved defrost for cold storage room refrigeration systems that operate at temperature (−20°C) conditions. To achieve this aim, the following goals were set:

1. We reviewed the literature to study the effect of frosting on the refrigeration systems dynamic, the performance of the system during the frost milting cycles, ways of defrosting in refrigeration systems, the advantages of control strategies in defrosting when necessary and numeric models for defrosting.
2. Design, construct and operate a test facility able to operate as a conventional defrost method Electric Heater Method (EHM) and as the New Defrost Method, and offer continuous monitoring of refrigeration system performance.

3. Search the effect of the NDM on the behavior of the refrigeration cycle, such as pressure change during the defrosting process, pressure ratio, sub-cooling, cooling efficiency, and power consumption. And compare it to the EHM.
4. Monitoring the cold storage room temperature throughout the system's operation period for both methods and decries the temperature fluctuation during the defrost process in the new method.
5. Evaluate the performance of the new defrost Method and its impact on the environment and economy by Energy, Exergy, Economic and Environmental (4E) analysis of both methods.

1.4. THESIS STRUCTURE

Part 1: This part addresses the introduction of the study. The first section clarifies the early refrigeration systems and their classification and a brief history of cold storage rooms and their uses. Then, it provides the motivation of study, from which the aims and goals of this study NDM are defined.

Part 2: Addresses Objective I, provides a literature review of the subject areas associates with the study subject *Defrost Method* including the impact of frosting on refrigeration system dynamics, system performance during defrost cycles, the demand defrost control strategies implementation and numerical models of the defrost process.

Part 3: Addressing Objective II, the chapter presents a comprehensive description of the experimental test facility that consisted of assembled cold storage refrigeration system, refrigerated compartment, cooling unit, and data acquisition instruments that were employed to monitor system performance.

Part 4: Addressing Objective III**,** this chapter provides a description of the experiment's procedure and the measurements recorded from the system in both methods and plotted the refrigeration cycles on the pressure/enthalpy diagram.

Part 5: Addressing Objectives IV and V**,** this chapter presents a thermodynamic analysis for refrigeration unit components as compressor work, evaporator capacity,

refrigeration efficiency, and applied the exergy analysis of the system to describe all energy losses in the system elements and the entire system.

Part 6: This chapter discusses the results obtained from experiments and theoretical analysis during the refrigeration process and defrosting process for new defrost and compare it to the traditional method (electric heater method).

PART 2

LITERATURE REVIEW

While Part one outlined the key issues associated with demand defrost on cold storage rooms refrigeration systems, the outline of Part two can be summarized as follows:

1. The numerous methods used to implement the defrosting process and evaluate theirs appropriately to different refrigeration systems.
2. The evaporator frosting effect on the refrigeration systems dynamics and performance.
3. The behavior of refrigeration systems through the defrosting cycle.
4. The adaptive demand defrosts strategies developed and conducted on many types of refrigeration systems.

2.1. DEFROSTING METHODS

Many methods were used to defrost the evaporator coil and sometimes more than one approach is used simultaneously. The most common approaches of defrosting methods which will be overviewed in this section are as follows:

- Off-Cycle Defrosting Method
- Electric Heater Defrosting Method
- Hot gas Defrosting Method
- Heated air Defrosting Method
- Water Defrosting Method

2.1.1. Off-Cycle Defrosting

Off-cycle defrosting is used where the temperature of the cabinet is maintained over zero degrees centigrade and a low amount of frost accumulation [10,11]. An off-cycle defrosting is as it sounds; defrosting is consummate by basically switching off the refrigeration process, stopping the liquid refrigerant from entering the evaporator. The evaporator temperature may be operating below zero degrees, however, the temperature in the refrigerated cabinet is above zero degrees. With switched off the refrigeration cycle, authorizing the air in the refrigerated cabinet to continue to circulate through the heat exchanger tube and fins will increase the evaporator surface temperature, occur the defrost. In addition, the normal air penetration into the refrigerated cabinet will cause the air temperature to increase, further supporting the defrost cycle. In applications where the air temperature in the refrigerated cabinet is normally higher than zero degrees, off-cycle defrosting proves to be an efficient approach for meltdown the buildup of frost from the evaporator and is the most common means of defrosting in cooling medium temperature applications. The compressor will continue operating to pumping refrigerant liquid out of the evaporator, to the low side, and in the liquid receiver. The compressor will turn off when the low pressure falls to the cut-out set point for the low-pressure switch. There is no other source of heat or energy that is necessary for an off-cycle defrosting. The system will be returning to the refrigeration process only after a period or limited temperature is reached. That limited temperature for the medium temperature application will be about 8℃ or 60 minutes if terminated by time. This process will be repeated up to four times per day depending on the refrigeration system manufacturer's recommendations.

2.1.2. Electric Heater Defrosting

The electric heater defrosting is a refrigeration process used in commercial systems and home refrigeration where the temperature of the cabinet is under +3°C [10,12,13]. During the electric defrosting, the fans of the evaporator and compressor motor are turned off. The series of electric heating components placed alongside the surface of the evaporator or even inside the evaporator tubes are energized. The temperature generating from the elements melts the accumulated frost on the evaporator tubes and

fins. Again, the condensate flows to the heated drain pan and it will be allowed to drain from the system. Although it is more customary on low-temperature applications, the electric heater defrost method also can be used on moderate-temperature applications. On low-temperature applications systems, the off-cycle defrost method is not suitable, needs more energy to milt frost on the evaporator that the air in the refrigerated cabinet is below zero degrees. When the defrost timer, clock energizes the electric defrost cycle, numerous things will happen at the same time. (a) A normally closed switch point in the defrost timer clock that supplies electric energy to the evaporator fans will open. This will switch off the evaporator fans, allowing the heat produced from the defrost heaters to be concentrated on the evaporator fins surface only, instead of transferring to the compartment air that would be circulated by the evaporator fans. (b) Another normally closed switch point in the defrost timer clock which supplies power to the liquid line solenoid will open. This will close the liquid line solenoid valve, to prevent the refrigerant to enter the evaporator. (c) Normally open switch point, in the defrost timer clock will close. This will also supply power directly to the defrost heaters. The electric defrosting method provides a more positive defrosting of energy than the off-cycle method, with faster durations. The defrost cycle will once again be terminated by temperature or time. Maybe there is a drop-down period after defrosting termination, a brief period that allows the water drops melted from frost to drip off the evaporator fins surface and into the drain tank. Additionally, the evaporator fans will be delayed from restarting for a short amount of time after the refrigeration process restarts. This is to ensure that any water drops still existing on the evaporator fins surface will not be blown into the refrigerated compartment. Alternatively, it will freeze and remain on the fins of the evaporator. The fan delay also decreases the amount of hot air that is circulated into the refrigerated cabinet after defrosting terminates. Fan delay can be accomplished by either a temperature control (thermostat or a time delay).

2.1.3. Hot Gas Defrosting

The hot gas defrosting method is commonly used in industrial refrigeration systems [14,15] especially in large refrigeration systems including display cabinets where the temperature degree is maintained to be less than −12°C [10], and in the air source heat

pumps [16,17]. During the cycle of defrosting, the refrigerated hot gas is directed from the compressor discharge directly to the coil of the evaporator heating the coil and melts the frost accumulated in its surface. The air cannot enter the refrigerated compartment because it is stopped by the evaporator fan or otherwise by closing the damper door on the supply air duct. The melted ice which is insulated from the coil is accumulated in the heated drain pan and can flow outside of the refrigerated compartment. This defrosting approach is characterized by its speed and simplicity and is presently used on entire trucks and trailer refrigeration systems [1]. The hot gas defrosts method uses the superheated refrigerant from the compressor discharge line (on high pressure and temperature) as the heat source. There are several kinds of hot gas defrost methods and all of them used additional valves to change refrigerant direction flows.

2.1.3.1. Bypass Defrosting

In this method vapor is diverted on a third system line, bypassing the condenser and the expansion valve, and directed through the unit cooler coil, warming it from the inside. The schematic below illustrates this concept.

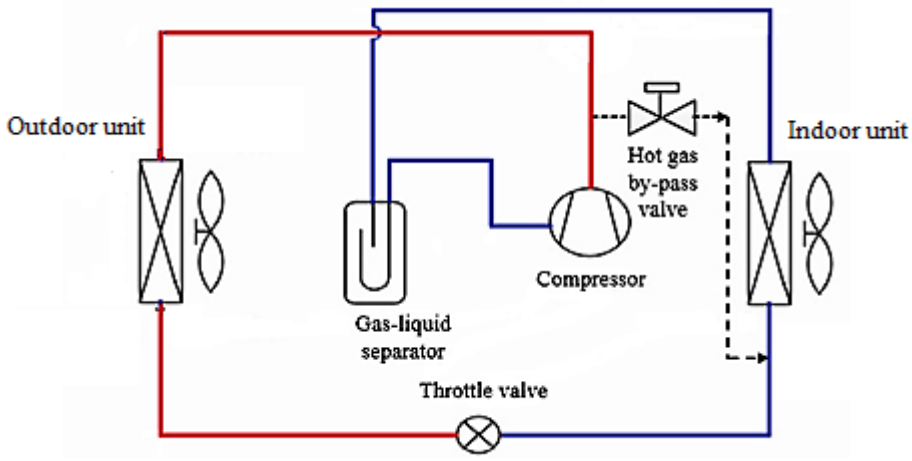

Figure 2.1. Schematic of bypass hot gas defrosting.

During the refrigeration cycle, the hot gas by-pass valve stays inactive by the controller or defrost timer, to allow the refrigerant to go through its regular path (compressor, condenser, expansion valve, and evaporator).

2.1.3.2. Reverse Cycle Defrosting

When the reverse cycle defrosting mode operates, its outdoor unit coil works as an evaporator while its indoor unit coil works as a condenser. During the defrosting process, the compressor pumps the hot gas to the coil of the evaporator to melt the frost. The control unit returns to its operation when the frost melts and drained far from the evaporator. It must be known that reverse cycle defrosting does not need any complex elements besides the four-way valve. This means that its system is simple and can be easily installed. The outdoor air provides the needed energy for reverse cycle defrosting. Its process is much shorter than the process that existed in hot gas bypass defrosting and this method of defrosting is commonly used as a standard method for defrosting in air source heat pump units for many years[18]. The schematic below (Figure 2.2) illustrates the direction of the refrigerant in reverse cycle defrosting during cooling and defrosting states.

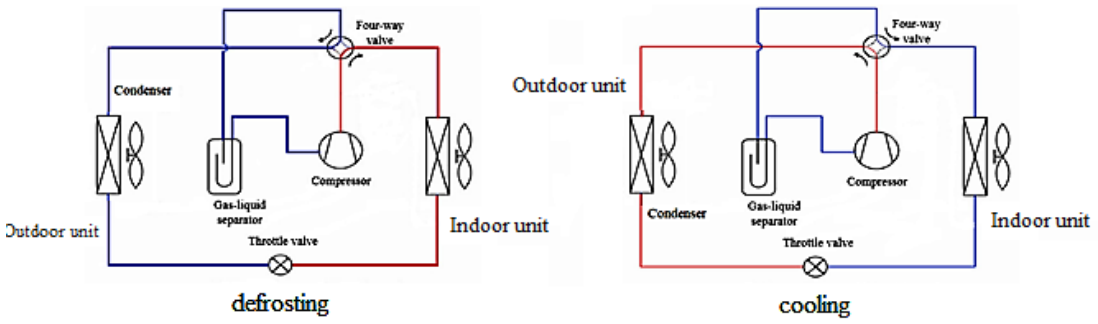

Figure 2.2. Schematic of reverse cycle defrosting method.

An experimental study on defrosting energy consumption and provision during the reverse cycle defrosting process for an experimental Air Source Heat Pump unit has been conducted by Dong et al. 2012. The practical results of the study exposed that the heat supply indoor air supported by 71.8% of total heat delivered to defrost and 59.4% of the delivered energy has been used for frost melting [19]. The highest efficiency of defrosting may reach 60.1% [20]. The performance of this defrosting method for an Air source heat pump unit an electronic expansion valve by the use two different control strategies: completely open and controlled by a DS (Degree of Superheat)

controller [20]. The experimental results of the study showed that a higher defrost efficiency is obtained when the EEV was controlled by DS controlled during the defrosting process. The refrigerant flow ratio was decreased during the last part of the defrosting process and therefore less heat was created and thus, it is noticed a higher defrosting efficiency and less heat loss.

2.1.4. Heated Air Defrosting Method

This type of defrosting method is mainly used in commercial systems where the temperature of the cabinet is maintained below −12°C with isolation to the air surrounding the evaporator [10]. During the defrosting process, the dampers which surround the evaporator coil are closed to isolate the coil from the refrigerated compartment. The air surrounding the evaporator coil is warmed by an energized heating element that is circulated to the coil melting the frost. The compressor stays off while the fans of the evaporator continuing rotating to fasten the heat exchange. This defrosting approach is not appropriate for some defrosting applications including the evaporator coil to transfer the refrigeration systems because of the difficulty to isolate the large evaporator coils from the compartment surrounds [1].

2.1.5. Water Defrosting Method

The water defrosting method is a quick defrosting evaporator method and is used in large industrial applications including warhorses and cold storage [1]. When the defrosting is started, the compressor and evaporator fans are stopped, and the water solenoid valve opens to allow the water to spray directly to the evaporator coils from a series of tubes locate over the evaporator. This type of defrosting method is considered a less acceptable substitute because the cabinet temperature reduces the freezing as water freezes on the heat transfer surfaces under specific circumstances [1], again make it unsuitable to defrost the evaporating coil of transfer refrigeration systems due to the extensive range of operating temperature in specific sub-zero Celsius temperatures [1]. The water defrosting system is pumping water into the evaporator when the cooling system is twisted off, this is operated manually or automatically. During the defrosting process, the evaporator blinds are closed. The

water is hot enough to liquefy the frost. Then it will flow into the drain tank. Drainage water should be coming out before the cooling unit is turned on or the water will freeze.

2.1.6. Defrosting Methods Summary

These defrost methods may be suitable in some refrigeration systems applications and are not suitable in others, for example, in domestic refrigerators electric heater method is used, and the reverse cycle defrost method is suitable in heat pump air conditioning systems, the efficient defrosting choices existing for the transport refrigeration units are hot gas defrost and electric heater defrost approaches [1]. In cold storage rooms, all defrosting methods can be used.

2.2. FROST GROWTH ON THE EVAPORATOR AND ITS IMPACT ON THE SYSTEM PERFORMANCE

Before embarking on the development of an enhanced defrosting system, it is necessary to be familiar with and understand the impacts of evaporator frosting on refrigeration system performance. Many studies and researches have been performed to examine the impact of coil frosting on refrigeration system performance and these studies are clarified in Table 2.1.

Table 2.1. Some of the earlier studies focused on frost growth and its effect on refrigeration system performance (1957-2018).

Author (s)	**The System**	**Key Findings**
Stoecker (1957)[21]	Refrigeration system coil	Through the continuous flow of air, the total heat transfer increased primarily because frost started to deposit and then decreased as frost thickness. The growth of frost causes a reduction in the airflow which drops the effectiveness of the system. The close fin spacing

		coils are more effective in the highlight of light frosting and the opposed is true with the accumulation of frost.
Neiderer (1976)[22]	Air cooler	The system performance and airflow are decreased because of the frosting. The wide and variable fin spacing of coils decreases the negative impact of frosting. The heat losses of the defrosting are ranging between 75 - 85%.
Fisk et al. (1984) [23]	Air-to-air heat exchanger	The accumulation of frost decreased the temperature efficiency. It is recommended for intelligent control systems to activate defrost only when needed.
Payne & O'Neal (1993)[24]	Air source heat pump	Through the continuous and higher airflow tests, the temperature has been maintained and increased time between defrosts. Low airflow decreased the times between defrosts and the temperature of evaporating.
Lee et al. (1996)[25]	Finned tube heat exchanger	The high temperature of inlet air caused a tinny high-density layer of frost. The environments with high humidity created a thick with low-density frost layer. The thermal performance of the heat exchanger is strictly associated with blockage rate whereas the heat exchanger with small fin

		space suffers more from the growing frost.
Stoecker (1998)[26]	Finned tube evaporator	With the accumulation of frost, the air openings size through the coil is decreased which increases the dropped pressure through the coil and increases the velocity of air through the coil.
Peng et al. 2003[27]	Air source heat pump	A small change in parameters of the heat pump until the frost layer accesses the critical thickness. The ratio of frost formation is highly affected by the airflow.
Aljuwayhel et al. (2008)[28]	Industrial evaporator coils	Frost formation effects of the low-temperature large-scale evaporator coil performance. The frost growth on the evaporator coil surface is negatively influenced by the resistance of airflow and the related drop in the air mass flow ratio.
Özen et al. (2014) [29]	fin-tube evaporator	Study the finned tube evaporator performance in the transient system numerically and experimentally. The results of the study showed that the values of frost thickness increase and the airside pressure drop with the increase in air temperature and relative humidity and the decrease in the whole conductivity values.

Sommer et al. (2016) [30]	Thermoelectric cooler (TEC)	Estimated the effect of surface energy on the density and frost thickness to both a hydrophilic substrate and a hydrophobic substrate. They discovered that the layer of frost on the hydrophobic surface is fluffier and thicker than the frost accumulated on the baseline surface.
Wu et al. (2017) [31]	Thermoelectric cooler system	They experimentally investigated the features of meltwater drainage and frost melting on the aluminum surface with the parallel and crossed grooves. The results of the study showed that parallel grooved surface characterizes by better drainage for meltwater than the flat surface and the capability to preserve a small ratio of it.
Da Silva et al. (2018) [32]	Review of frost measurement methods for demand defrost	If the frost leaves to continue the accumulation, the efficiency will continue its decrease because of an increase in heat transfer resistance between the fins which cause a complete blockage if not applying the defrost process.

Many researchers studied the growth of frost on evaporators and its influence on the performance of refrigeration systems. The influence of frost formation on heat transfer coefficient surface for the refrigeration systems coils have been studied by Stoecker, 1957, the result of the study showed that the total heat transfer of coil first increased by 5 to 6% at the first two pounds of frost and then decreased when the mass of frost is increased [21]. The efficiency of the refrigeration unit is decreased due to a decrease

in airflow because of the defrosting. When the accumulation of frost was light, the coils with close fin space (nine fins per inch) were more effective but the opposed is true because the frost accumulates due to the large drop of airflow in closely spaced fins. The coils which consist of broader fin spacing are more effective under the frosting circumstances, a study has been performed by Niederer, 1976, to determine the influence of frost builds up on the evaluated capacities of air coolers and various fin separating designs. The results of the study showed that the frost builds on the heat transfer surface of the fins decreased the airflow and therefore decreasing the effectivity and capacity of the system which confirm the prior observations [22]. The air cooler capacity which characterizes by broader fin spacing (four fins per inch) was lesser influenced than those with closer fin spacing (six fins per inch). Consequently, they may work for longer periods with higher effectivity between defrosts [22]. Moreover, the air coolers which include variable fin spacing were less influenced than the traditional constant fin coils with the same level of frost buildup. As well as, it is showed that during defrost only 15% to 25% of the temperature needed to defrost has been removed with the condensate. The remaining percentage (75% to 85% has been lost in the surrounding environment of the unit to heat the air cooler cabinet and the coil metal. A heat exchanger and the fin spacing is 4 fins per inch (1.6 fins per cm), relative humidity is 72% and inflowing air conditions is 0°C have been represented by [26]. The pressure drop through the heat exchanger increases when increasing the speed of air and the accumulation of frost. When the frosts accumulate, the air passage across the coil decreased which results in an increase in the pressure drop across the coil and increases the air speed across the coil. Therefore, it is proposed that the initiation of defrosting is based on increasing the pressure drop through the evaporator or on increasing the air speed across the evaporator. Both of them witness an increase in the frost buildup.

A practical study conducted by Fisk et al. (1985), on the performance of two residential air-to-air heat exchangers (one of them is crossflow and the other one is counter-flow) under periodic defrosts and freezing conditions. The results of the study showed that the efficiency of the crossflow heat exchanger reduced at the ratio of 1.5 to 13.2 percentage points per hour when the frost and ice accumulate [33]. A quicker reduction in the efficiency of the heat exchanger was related to shorter freezing

periods, higher warm air stream humidity, and lower cold air stream temperature. The efficiency of the counter-flow heat exchanger is decreased at a slower ratio (0.6 to 2.0). The reason behind this is due to the larger flow passages and as much of the condensed water was drained to the warmer place of the coil where it may not be frosted. The defrost time fraction (defrost time divided by the defrost time and total freeze) did not highly differ between the two heat exchangers and ranging between 0.06-0.26. As well, the researcher recommended developing a freeze protection system (defrost control system) which may: i) the freeze protection is activated only at necessity, ii) adjusting the change in flow ratio, indoor humidity, and outdoor temperature in an automatic way, iii) it is not activated by the performance of changes resulting from other elements rather than frosting and, iv) it removes the need to conduct extensive tests for each unit under the freezing circumstances.

The impacts of outdoor fan airflow ratios on the frost/defrost cycle of the air source heat pump have been investigated by V. Payne & O'Neal, 1992, in an interesting study. The basic tests have been performed with normal airflow of 72 m^3/min which was allowed to reduce frost formation on the evaporator. Moreover, they performed airflow tests by the use of booster fan to maintain the airflow when the frost accumulated on ten evaporator coils whereas the high and low airflow tests were particular airflow ratios of 40 and 88 m^3/min that allowed to decrease with frost buildup. The results of the study can be summarized as follows [34]:

- Decrease the airflow in the basic case caused a decrease in the evaporating temperature.
- The constant airflow case created cycle time which was longer by 43% than ten basic cases whereas defrost time was longer by 14% only.
- The test of constant airflow maintained a constant evaporating temperature whereas at the same time delay the degradation of air to refrigerant the heat energy transfer.
- The temperature capacity of the constant airflow test decreased by less than 5% and this refers that the airflow is the leading element in the performance of heat transfer during the frosting with the insulting impacts of the secondary frosting layer.

- The tests of higher evaporator airflow presented an increase in heat pump heating capacity, delay in the degradation of evaporating temperature and therefore, cycle time is increased by 31% whereas the defrost times increase by 12.5% only.
- The test of lower evaporator airflow unexpectedly produced reduce of 36% in the cycle times with 58% less condensate collected through the succeeding defrost cycle. The rapid growth of frost is due to the decreased evaporating temperature produced from the lower airflow ratio. The whole defrost cycles of the four test cases provide have been ended when the temperature of the lowest liquid line circuit of the outdoor heat exchanger accessed to 26.7°C.

The frost formation impacts on finned-tube heat exchangers have been experimentally studied by Lee et al. (1996). This study was conducted on a 2-column and 2-row finned-tube heat exchanger and investigated the heat exchanger design element's impacts (fin arrangement and fin spacing) and operating circumstances (airflow, humidity, and temperature) on the growth of the frost layer and heat exchanger performance. The findings of the study showed that increasing the air temperature will form a frost layer with a thin thickness and high density. When the humidity of the air inlet increases, the thickness of frost increases, the density of frost increases, and energy transfer resistance increases. Nevertheless, the thermal resistance is decreased when increases the airflow but leads to an increase in the thickness and density of frost [25]. As well as, the researchers clarified that the heat exchanger thermal performance is highly associated with *"blockage ratio"* and can be defined as the airflow passage rate blocked by the frost layer. Moreover, the study detected an important change in heat transfer ratio with coils characterized by thin fin spacing (5 mm fin spacing) where the frost is developed compared to coils with big fin spacing (20mm fin spacing) where there is a small change in heat transfer with frost accumulation. These results came consistent with ten results obtained by [21,22].

The operating features of air source heat pump behaver have been studied by Peng et al. (2003). The study conducted on nominal capacity is 70kW heat pump during the frosting and defrosting circumstances, clarified that during the frosting phase, there was a little change in most of the thermal pump factors until the frosting

layer thickness reached 0.24 mm and this factor has been proposed as a trigger to start the melting. When exceeding this critical value, the operating features of the heat pump were changed with compressor discharge and suction pressures increased and decreased respectively. Despite the change in compressor pressure with frost accumulation, the power of the compressor remained constantly virtual. The formation and accumulation of frost were highly affected by the average airflow [17]. The formation of frost started earlier, and the thickness of the frost layer increased quicker with lower airflow ratios (50% of the nominal airflow), and this is similar to the results obtained by W. V Payne & O'Neal, 1993. The heat pump cycled on\off through the defrost cycle because of the particularly low suction pressure. The system design upgrade where introduced and tested which include a duct with a solenoid valve that connects the receiver with the suction side of the compressor. A small part of high-pressure gas was provided to the suction side of the compressor through the defrosting process that prevented the cycling of heat pump on\off and leads to enhance the defrost cycle [24].

The effect of frost accumulation on the performance of a low-temperature large-scale evaporator coil which is commonly used in commercial refrigeration systems experimentally studied by Aljuwayhel et al. (2008). They performed many experiments to identify the evaporator capacity of in-situ coil refrigeration on time where the frost accumulates on its surface. They performed many field measurement quantities such as outlet and inlet air relative humidity, air volumetric flow ratio, and outlet and inlet air temperatures. Also, they measured the effect of frost accumulation on low-temperature large-scale evaporator coil performance. The frost formation on the evaporator coil surface caused an increase in the airflow resistance and related drop from in the air mass flow ratio. The temperature drops of the air as it passes through the evaporator coil will increase as a result of the leaving air temperature decreasing. The decrease in air mass flow ratio causes a monotonically decrease in the evaporator cooling capacity [28].

The performance of the finned tube evaporator at the transient regime was investigated by Özen et al. (2014), for both experimental and numerical study. The results showed that increasing the relative humidity and air temperature will drop the air side pressure

and increase the values of frost thickness whereas the values of total conductivity are decreased. The drop-in inlet air temperature is increased the total conductivity. At the same relative humidity, an increase in the air temperature causes an increase in air humidity. An increase in air humidity will lead to an expansion in the thickness of frost and therefore cause a decrease in total conductivity [29]. Since its spongy medium includes ice crystals and pores filled with moist air, the formation of frost on the evaporator's fin surface increases the thermal resistance of the air-side and decreases the effectiveness and capacity of the system. The frost is allowed to grow up continuously which decreases the efficiency not only because of the heat transfer resistance increases but besides the blockage where the passage of air can be completely blockage if do not apply frost method [35].

An experimental study conducted by Da Silva et al. (2011), on the impact of frost formation on the thermo-hydraulic performance of tube-fin evaporator coils. The results of the study showed that the ratio of frost formation is increased with the fin density, airflow ratio, and sub-cooling value in the liquid line. The study concluded that the airflow ratio is the most important element to the evaporator drop capacity [36].

To predict the outdoor unit performance Ye & Lee, 2013, conducted their study by taking into consideration the decrease of airflow ratio because of the frost accumulation, and the numerical model of the study has been validated and enhanced. The study concluded that the convective thermal resistance between the air and frosty surface results in 90% of the entire thermal resistance and that the conductive thermal resistance from the tube wall to the frosty surface is just 2-5% of the entire resistance. Moreover, the increase of the convective thermal resistance from the frosty surface to the air is highly different as a blockage rate function because of the accumulation of the frost layer [37].

An experimental study about the accumulation of frost on the louvered creased fins in outdoor unit microchannel heat exchangers. the study on air source heat pump systems was carried out by Moallem et al. (2013). The results of the study showed that for louver fin variation of the fin width were not highly enhanced the frosting performance

of the fins but increasing the depth of fin seemed to increase the capacity of the fin (39%) with the existence of several penalizations to the time of frosting (6%) [38]. In addition, the fins capacity enhanced up to 53% when the airspeed increased from 0.8 m/s (157 fpm) to 1.6 m/s (315 fpm).

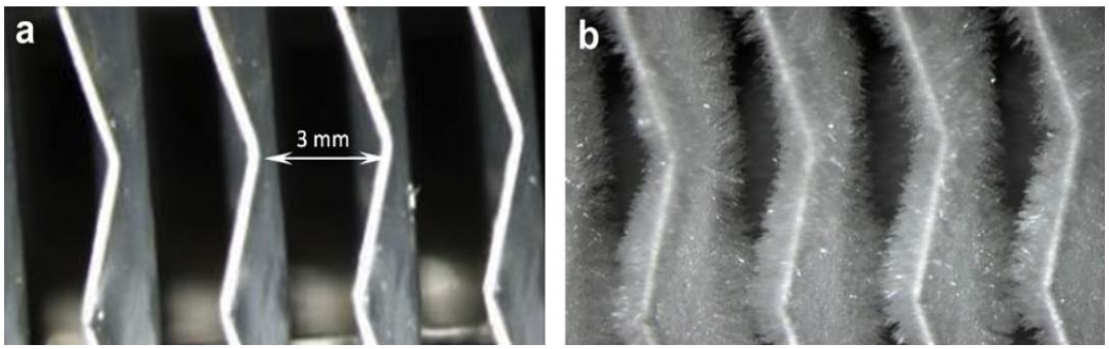

Figure 2.3. Visualization of the fin surfaces before (a) and after (b) the frost formation process [36].

The frost melting, the condensation and accumulation of frost crystal, and features of meltwater drainage on the aluminum surface with crossed and parallel grooves have been studied by Wu et al. (2017). The results showed that the worse drainage of meltwater is in crossed grooves while the surface with better drainage is in parallel surface followed by the drainage on a flat surface with a small meltwater retention rate [31].

Sommers et al. (2016), detected that the correlation of present frost density does not include the wettability of the surface as a parameter in the model. Nevertheless, the wettability of the surface is very significant to verify accurately the frost layer properties and therefore must be consistent in future frost correlation development studies. The authors assessed the impact of surface energy on density and frost thickness to both hydrophilic substratum and hydrophobic substratum and detected that the frost layer on the hydrophobic surface is fluffier and thicker which result in less thick frost if compared with baseline surface frost [30].

2.2.1. Frost Growth on the Evaporator and Its Impact on the System Summary

The experimental studies which have been conducted independently highlighted several common results in terms of the effect of frost on systems performance and these results can be summarized as follows:

1. Coils with broader fin spacing conduct better under frosting circumstances comparing with coils with closer fin spacing [21,22,26].
2. The airflow ratio through the coil has an important effect on the frost formation ratio [17, 27, 26].
3. Through the early phases of frost accumulation, a little increase may have resulted in the performance of thermal transfer but with the continuous frost accumulation, the airflow decreases in addition to the efficiency and capacity of the system [21].

However, the defrosting process should start before the evaporator loses 10% of its capacity, as shown in Figure 2.4, to maintain airflow, capacity, and efficiency at a high level. Moreover, defrosting methods need energy and time, which affect system performance [7]. Therefore, a new method is proposed in this research to defrost an evaporator that uses less energy and time.

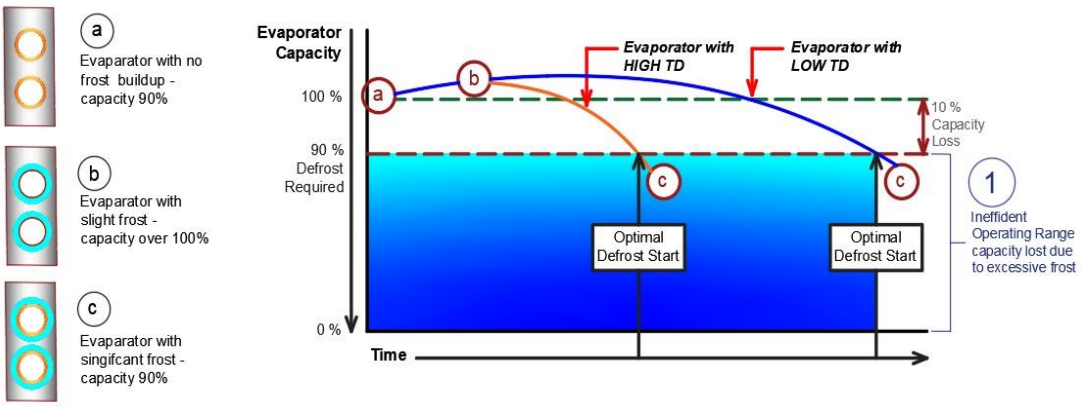

Figure 2.4. Effect of the frost accumulation on the evaporator and heat transfer [7].

2.3. REFRIGERATION SYSTEM PERFORMANCE DURING DEFROST

While at the previous part we summarized and displayed studies and researches which outline the impacts of frost accumulation on the behavior of refrigeration systems, this part of the study will focus on the refrigeration system behavior during the defrost process whereas system performance under both frosting and defrosting is of interest in the Refrigeration System *Defrost* study. Table 2.2 summarizes the main results of related literature followed by a more detailed review.

Table 2.2. Summary of some studies on refrigeration system performance during the defrosting process and efforts to improve (1983-2020).

Author (s)year	**Refrigeration Systems**	**Study and Results**
Stoecker et al. (1983)[39]	Industrial refrigeration system	Decreased the requirements of energy during the defrosting process by providing the least amount of hot-gas pressure to accomplish acceptable defrost. The thermal energy was used to heat coil and frosting, melting, and warming. The higher refrigeration temperature and flow ratios decrease the efficiency of defrosting.
Strong (1988) [14]	Industrial refrigeration system	The determined optimal sequence of events to defrost the evaporator coils. The significance of adequate quantity but not excessive amounts of hot gas refrigerated to cover the losses and enhance the frost effectivity. The best selection is the defrosting on demand.
Cole (1989) [40]	Industrial refrigeration system	Generally, 80% of the necessary energy to defrost the evaporator coil returns to the refrigeration system as added load.

		The highest defrost effectivity is amounted to 60% to 75%.
Al-Mutawa et al. (1998) [41]	Industrial refrigeration system	Calculations of heat load, data gaining system, and experimental test facility description. Outlines about the dynamics of the system during the refrigeration and defrost cycles and the quantitative data on heat loads related to the defrosting coils.
Ozyurt et al. (2002) [13]	Domestic refrigerator	Domestic refrigerators are provided by two evaporators and each one of them is arranged in the parallel and serial method. The efficiency of defrosting has amounted to between 13% and 65% for the freezer and fresh food evaporators with heater defrost feature. With the combination of air and heater defrost, the efficiency of fresh food evaporator defrost is between 70% and 100%.
Dong et al. 2012 [42]	Air source heat pump	71.8% of total heat supplied for defrosting comes from the indoor unit and 59.4% of the supplied energy is used to defrost. The efficiency of the highest defrost may be reached to more than 60.1%.
Long et al. (2014) [43]	Air source heat pump	Enhanced the defrosting approach by the use of both the reverse cycle approach and the new reverse cycle defrosting approach. The results of the study showed that the time of defrosting is decreased by 65% and that the total consumption of energy is

		decreased by 65% if compared with the reverse cycle approach. Moreover, the new reverse cycle method guaranteed continuous heating during defrosting. Compared to the reverse cycle method, the input power and total heating capacity are raised by 12.6% and 14.2%, respectively.
Ghadiri et al. (2016) [44]	Domestic refrigerator system	Modified a defrosting method by taking into consideration the effective processes such as heater action before, previous defrost time, compressor ON time, compressor fans style, and open-door time. The results of the study showed a reduction in consumption of energy by 13% and a total equivalent warning effect by 12.5%.
Kim et al. (2016) [45]	Heat exchanger	Studied the drainage and thermal performance of asymmetric and symmetric louvered finned tube heat exchangers during the frosting and defrosting circumstances. The study results showed a decrease of more than 17% in the total heat transfer ratio of the symmetric finned tube. Instead, through the new asymmetric fins, drops of water have not been seen over the leading edge of the fins after the defrosting operation.
Zhao et al. (2017) [46]	Domestic frost-free refrigerator–freezer	The airflow across the evaporator and leaking to the freezer while the phases going on and therefore increases the freezer temperature

Yoon et al. (2018) [47]	conventional household refrigerator	Suggested three methods of defrosting for no frost refrigerators and these methods including simple pulsating mode, individual pulsating mode, and sheeted heater power control. The results of the study showed that all of the three methods are efficient in increasing the defrost efficiency and increase the temperature of the freezer. Nevertheless, the best performance has been achieved through the individual pulsating mode.
Liu et al. 2018) [48]	Domestic refrigerator system	Proposed a new defrosting method by the use of outdoor air. The experimental study included different temperature ranges between (0 - 45°C). The results of the study showed that the consumption of power for outdoor air defrosting is 77.6 - 98.2% less than that of the electric heater defrosting system through the same defrosting time.
Wang and Zang (2018) [49]	Cold storage room	Adopted the liquid refrigerator to defrost the evaporator by the use of eight solenoid valves and two evaporators. The results of the study showed that the power compressor reduced by 60% from 2.0 kW to 0.8 kW and the deforesting operation buildup without any extra energy.
Zheng et al. (2019)[50]	Air source heat pump	Proposed a new defrosting method that depends on image processing to avoid the mal defrosting process (Temperature Humidity Image)

		approach. The results of the study showed that the unnecessary and late defrosting occurrence is certainly found under (Temperature Time) approaches because of the disability of direct control information, whereas the Temperature Humidity Image approach might identify the frost layer accumulation directly.
Zhao et al. (2020) [51]	Household frost-free refrigerators	Adopted a fan cover opened during the cooling process and closed during the defrost process to prevent warm air intrusion passage to cold space. Results show that defrost duration was reduced by 4.5min and temperature fluctuation was reduced by 2.7℃
Malik et al. (2020) [52]	Domestic refrigerator	Proposed a novel hybrid frost detection system that includes a new photo-capacitive sensing technique and double purpose besides defrosting heater and manufactural sensor. The system can reveal the frosting shape and measure its thickness from 1.3 to 8 mm with a 5% error margin.

Stoecker et al. (1983) established features throughout the laboratory experiments which can decrease the requirements of energy through the hot gas defrost cycles of industrial refrigeration systems. The conducted studies are as follows: i) the least hot gas to accomplish reasonable defrost; ii) an approach to drain the condensed liquid of the evaporator coil; iii) the accurate time to finish the defrost cycle. The study suggested a hot gas pressure of 15 psi over the controller of outlet pressure to the ammonia and R22 tested systems. They identified the thermal energy which is used during defrosting and included necessary energy to heat condensate, warm fins and

tubing, and frost melting. As well as, it is detected that defrost inefficiency is normally low when employing the pressures and refrigerant flow ratios. The defrost effectivity has been defined as “the rate of the total heat necessary for defrosting such as the reasonable frost warming to the entire amount of deforesting temperature comprising any impacts of refrigeration loads” [53]. Strong, 1988, has been defined the optimal sequence of events that must be used during the defrosting elaborator coils process in the industrial refrigeration system [14] as i) the liquid from the evaporator is removed, ii) the air circulation fan is turned off, iii) hot gas defrost is conducted, iv) the hot has refrigerant is removed, v) the evaporator coil is re-col and the fan off and vi) the refrigeration is resumed with the fan on. As well as, the study clarified the significance to supply an adequate amount of hot gas to cover the losses of pressure and heating and both of them are basic elements to enhance defrost efficiency. Moreover, the study showed how demand defrosting is eventually the most efficient method to decrease the operating cost and conserve energy. The refrigeration loads and related hot gas defrosting costs for the industrial refrigeration systems studied by Cole, 1989, and The results of the study showed that more than 80% of the energy necessary to defrost the evaporator is usually returned to the refrigeration system as added load [40], and this result is consistent with the results of [22] which have been shown in Table 2.1. This is caused defrost efficiency of less than 20%. Based on the size of coil, materials, and configuration, the highest feasible deforest efficiency was approximated at 60-75%. In addition, the study identified two basic methods through which losses have occurred including heat and mas air transfer to the refrigerated vapor and refrigerated space bypass to the compressor part [40]. A series of five papers that clarify in detail experimental study to obtain quantitative and reliable data about thermal loads associated with hot gas defrost for industrial freezers coils offered by Al-Mutawa et al. (1998) the first two papers provided the experimental test, devices, and data obtain system. The third paper provided the test procedures and methodologies to decrease the data used to identify the thermal loads. The fourth paper presented graphical test data for the key variables during the frost and defrost cycle to identify the dynamic behavior of the system. The fifth paper presented quantitative data related to thermal loads which associate with hot gas defrost of the industrial coils [41]. Some researchers Identify the quantity of heat energy used through the industrial refrigeration coils defrosting as [39] [40], and [41]. A study uses both heater and air

defrosting defrost many permutations to ensure the effectivity of defrost cycle in domestic refrigerators with double evaporators. The study clarified that defrosting represents about 10% of the total consumption of energy in the refrigerator of type no-frost and therefore decided to focus on the alternative defrosting method. It is shown that air defrosting in the fresh food compartment is not suitable for serially connected double evaporator refrigeration cycles because of the defrosting cycle period and unacceptable temperature increase in the frosting compartment. Defrosting of parallel-connected double evaporators was the most effective method for defrosting for the fresh food compartment whereas the frosting compartment continued in cooling. The defrosting efficiency of evaporators has been calculated as 13% and 65% of the fresh food and freezer compartments with defrosting in the heater, respectively. In terms of the defrosting and heater combination, the defrosting efficiency ranged between 70-100% for the fresh evaporator. While air defrosting is an option for defrosting of evaporators in compartment fresh food of domestic refrigerators, this is not possible for transport cooling systems because of subzero Celsius operating circumstances and long periods associate with air defrosting. Moreover, the efficiency of defrosts of domestic refrigerators differs from the efficiency of transport refrigeration systems because of different defrosting approaches used and the high difference in both system's capacity. An experimental study provided by Dong et al. (2012), about the energy consumption of defrosting during the reverse cycle defrosting operation of the air source heat pump unit, was conducted and reported. The indoor unit fan has been turned on to provide a high amount of temperature for a short period of defrosting through the defrosting cycle. The findings of the study showed that the amount of heat supplied from the indoor air participated by about 71.8% from the total heat supplied for defrosting and about 59.4% of supplied heat is used for defrosting. The maximum defrosting efficiency was reached 60.1%. The reverse cycle defrosting approach is usually used for air source heat pump defrosting. Nevertheless, the air heating is interrupted by this process during the defrosting operation. At the defrosting cycle end, a time lag happens to restart the heating process. Furthermore, the repeated switching of the four-way valve may expose mass leakage to the refrigerant and negatively affect the performance of the unit. In addition, the compressor shell causes some dissipation of the heat to the atmosphere [19]. The study used this dissipated heat and enhanced the defrosting process. During the defrosting process, the heat wasted by the

compressor heats the space. The experiments of study used both the novel reverse cycle defrosting method and the Reverse Cycle method and were performed on the Air Source Heat Pump unit of an 8.9 kW heating capacity. It is shown that in the novel reverse cycle method, the pressure of discharge is increased by 0.33 MPa and suction pressure is raised by 0.14 MPa, the defrosting process period is restricted by 65% whereas the restarting heating period is missed with the new method and that the total consumption of energy is decreased by 27.9% if compared with reverse cycle method during the operation that is separated to defrosting period and resuming heating period. As well, the new method guarantees continuous heating during the defrosting process. The difference of temperature among the inlet air and outlet air of the indoor coil accesses to 4.1^{o}C during the defrosting process. During the experiment, the period reached 125 minutes comparing with the Reverse Cycle method, the input power, and total heating capacity are raised by 12.6% and 14.2% respectively. The system COP is increased by 1.4%. Kim et al. (2016) investigated the thermal performance and drainage of the asymmetric and symmetric louvered fin heat exchanger during the periodic frosting and defrosting circumstances [45]. The findings of the study showed that during the symmetric louvered fin that is considered a conventional defrosting design, the water formed after the defrosting process is kept on the leading edge of the fin and forms a bridge between the fins. The existence of these drops will cause an increase in air-side pressure drop in the frosting process. Consequently, the symmetric louvered fin decreased the total heat transfer ratio by 17%. In contrast, the new asymmetric louvered fins do not include drops on the leading edge of fins after the defrosting process cycle. So, the heat transfer ratio of the heat exchanger which exists in asymmetric fins was 10% greater than that exist in symmetric fins after the third cycle. They supposed that high drainage in asymmetric fin was because of the decrease in surface tension between the water drops and fin surface. In order to study this assumption, they compared the surface tension according to the fin's geometry by the use of enlargement models of the fins leading edge. They detected that the surface tension in the leading edge of the symmetric fins was 11% greater than that of the asymmetric fins that lead to enhancing the performance of drainage in the asymmetric fins.

Ghadiri Modarres et al. (2016) enhanced the defrosting process efficiency by proposing a defrosting approach to defrost the evaporator in domestic refrigeration systems. In the proposed technique, parameters including compressor fans mode, preceding defrost duration, heater action before, during, and after defrosting, open-door time, and compressor ON time was considered efficient on defrost procedure. The experiments were implemented on two different status study top-mounted freezers. The results of the study showed that for status one, it is indicated that the adaptive defrost in comparison to the fixed defrost cycle may decrease the Total Equivalent Warming Effect by 12.5% and the consumption of energy by about 13%. The same parameters for the status study two were decreased the Total Equivalent Warming Effect by 5.2% and consumption of energy by 5.5%. Moreover, the temperature fluctuation of the air of the compartment in both studies has been decreased if compared with the corresponding base case, which inhibits the food from losing its quality during the defrosting process. All in all, the findings of the study referred that more environmentally friendly impacts, decrease the consumption of energy and decrease the fluctuation in compartment air temperature [44].

The impact of defrosting heat leakage to the freezer temperature increase through the continuous defrosting process in a No-frost refrigerator–freezer has been experimentally studied by Zhao et al. (2017). The type of defrost heater was a tabular metal-sheathed heater installed in the upper part of the evaporator. The defrosting process includes three phases including worming, melting, and draining. The results of this study showed that during the defrosting process from the bottom to the top of the evaporator, the adjacent fin flow area is gradually enlarged. Therefore, the continuous stages witnessed the flowing of more warm air over the evaporator and leak to the freezer which increases the temperature of the freezer quickly. This result gives instructions to decrease the freezer temperature through the defrost cycles of the frost-freezer refrigerator-freezer. First, in the drainage phase, the freezer temperature most rapidly increased, thus reducing the heater power in this phase may relieve the temperature leakage, therefore decreasing the freezer thermal increase. Second, it is noticed that defrosting was much unsynchronized in the vertical direction of the evaporator. Frost has been removed from the bottom rows eight minutes before that in the top rows. This may help in extending the defrosting process period, promote the

increase of freezer temperature, and therefore, methods to shorten this time gap may contribute to reducing the increase of freezer temperature [46].

Yoon et al. (2018) suggested three defrosting methods for a No-frost refrigerator: the simple pulsating method that controls the two heaters together at the same time, the party pulsating method that controls every heater alone, and the supply energy method to a sheathed electric heater (radiation heater) in steps. Enhancement has been conducted to reduce the increase of temperature in the freezer and increase defrosting efficiency. The study findings showed that all of the three methods were efficient to prevent an increase in freezer cabinet temperature and increase defrosting efficiency. Nevertheless, the individual pulsating method provided the best performance where the defrosting process efficiency was enhanced by 15% and the fluctuation of temperature was 5.0°C only. In the individual pulsating method, the heater power is more professionally controlled by controlling both of the heaters alone different from the simple pulsating method. The impact of the sheathed electric heater ratio was the most significant element on the freezer temperature. It was efficient to apply the power constantly to the distributed heater (conduction heater) until completing the defrosting process. Temperature-feedback heater control that is not considered a conventional defrosting method helped to avoid increase the temperature of the freezer cabinet through the defrosting cycle and thus improved the defrosting process efficiency. This process may show good performance in power conservation [47].

Liu et al. (2018) developed a new defrosting technique by the use of outdoor air to defrost the evaporator. As shown in Figure 2.12, the authors used an electric heater and outdoor air circulation for anti-condensation to compensate for temperature in the cold cabinet heats. The experimental study has been implemented on the domestic refrigerator to different ambient temperature ranges of (0 to 12°C, 12 to 22°C, and 22 to 45°C). The study findings showed that the consumption of energy for outdoor air defrosting is from 77.6 to 98.2% less than the electric defrosting systems under the same defrosting time [54].

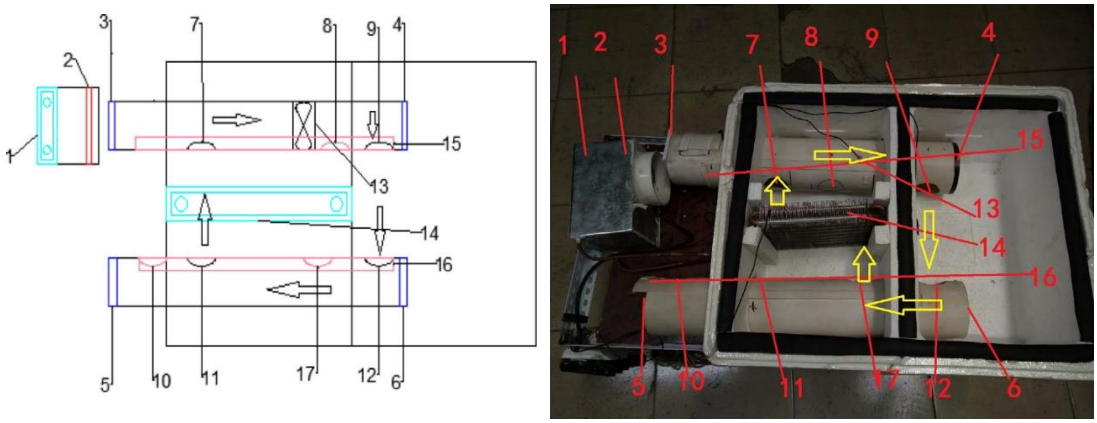

Figure 2.5. Schematic of the defrosting operation of the refrigerator with DSUOA [54].

Wang & Zang, 2018, improved a defrost method that using the liquid refrigerant heat, their method leads the high-pressure liquid refrigerant in the receiver to defrost the evaporator. During the defrosting process time, the refrigeration cycle is continuous at half capacity with no additional consumption of energy. The findings of the study showed that the compressor power decreased by 60% from 2.0kW to 0.8kW and defrost accumulates without any additional energy. The power has been highly changed. The use of a constant frequency piston compressor through the frosting and defrosting process decreases the LRD system performance. The experiment can be implemented with two compressors parallel and just one compressor can be used during the defrosting process with a variable frequency compressor [49].

A new defrosting control system depending on image process technology for Air Source Heat Pumps was proposed by Zheng et al. (2019), to avoid unneeded defrosting cycles. They implemented the control logic of the Temperature-Humidity-Image (T-H-I) method and analyzed the image processing technology technique. To evaluate the defrosting degree, they used the frosting coefficient. In addition, they determined the optimum standard judgment frost-defrost. Six typical experimental cases were implemented to check the advantages, applicability, and possibility of this method in a controlled experimental compartment. They studied both the Temperature-Time (T-T) control method and the performance of the T-H-I control method. The findings of the study were implemented as follows [50]:

1. The traditional T-T control method unavoidably caused the mal-defrosting phenomenon in typical environments because of the lack of direct control system information. In the environments characterized by medium temperature and high humidity, under which the frost accumulated easily and deposited rapidly, delayed defrosting has been detected. With the environment with low relative humidity and low temperature, which were typically unwanted conditions for frost accumulation, unneeded defrosting cycles were shown.
2. The suggested T-H-1 method may lead to reasonable and more precise defrosting decisions and therefore competitive performance to avoid mal-defrosting cycles. The needed defrosting process was begun at the right time before the ASHP performance quickly deteriorated and the ASHP switched to the heating process with frost film and residual water nearly milted and evaporated.
3. The image processing technique confirmed clear benefits to determine the frosting status. The image pre-processing improves the quality of the image. The frost visual properties have been measured by image multi-threshold segmentation and greyscale transformation technique. In order to increase the accuracy of frosting degree assessment, non-frosting area, medium frosting area, and high frosting area have been distinguished.
4. The frosting coefficient P difference may describe the frosting degree on the fin surface efficiently. P enhanced slowly in the frost nucleation time, provided a comparatively sharply upward trend during the frost layer accumulation period, and increased gradually during the full frost layer accumulation period. During the defrosting process, P provided a quick increase and finally remained under 0.05 until the defrosting cycle end.
5. The frosting coefficient P was introduced to evaluate the degree of frosting the optimal criterion judgment for defrosting opening (P1=0.3) and end (P2=0.05) were applicable in different environmental circumstances. Defrosting quality has been quantified depending on gotten images and previous research results.

By denoting and comparing the frosting process and processed images of compatible time, accurate defrosting decisions were detected in typical experimental cases. By taking into consideration the promising application's prospect of the T-H-I method to

avoid the mal-defrosting process, it is necessary to consider the following analyses for future researches:

a) Conducting more studies to analyze the system performance and energy-saving advantages of the T-H-I system through the heating process and compare these results with other methods.
b) Summarize the optimal criterion judgment of the frost-defrost process of different fin categories.

Zhao et al. (2020), suggested comprehensive measures in order to enhance the electric heater defrosting performance in household frost-free refrigerators. They used a fan cover that closed during the defrosting process to prevent warm air intrusion passage and opened during the cooling process to provide cold air to the compartment. Moreover, another heater (60W) has been placed in the middle height of the evaporator in addition to the original one (180 W) to match a better form of the frost heat. The study findings found that the double heaters in addition to the fan cover increased the temperature of the free compartment by 2.7℃ and reduced the defrosting period by 4.5 min [51]. Decreeing the freezer compartment temperature after the defrosting process led to more decrease in power consumption for the following recovery process, which compensated for its increase of the defrosting process and dominated the 1.2% increase in total power consumption of the refrigerator. Both of these measures proved effective in enhancing the defrosting performance. Nevertheless, the effect of the middle heater in cooling the cycle performance of the refrigerator needs further studies [49].

A new hybrid frost detection and defrosting system (HFDDS) for household refrigerators have been improved by Malik et al. (2020), using an arrangement of photoelectric sensing, resistive heating techniques, and capacitive sensing. The frost detection system is comprised of a capacitive sensing method (CSM) and an infrared (IR) based optical coupler. The additive cathode AMC and the refrigerator evaporator coils have been used as an equivalent plate capacitor for capacitive sensing. AMC has been used as a weak electrical conductivity and manufactured from a graphite-based polymer compound and allows to use of AMC as a resistive heater in the defrosting

process. The frost detection range of HFDDS is surrounding between 1-8 minutes with error tolerance amounted to about 5%. When the critical thickness of frost is reached, the HFDDS activates the defrosting process. The type of application determines the critical threshold. The enhanced HFDDS is characterized by flexibility which allows using of application-specific geometries of capacitive and photoelectric sensing units. Furthermore, the study findings showed that the additive manufactured graphite-based heating elements may be used as a low-energy defrosting process in a domestic refrigerator [52].

2.4. LITERATURE REVIEW SUMMARY

The literature review shows that numerous studies searched the impacts of evaporator frosting on the system performance. The shared subject arising from the previous studies agrees that with the frost accrues on the evaporator coils, the free airflow space through the coil reduces and thus decreases the airflow through the coil. A lower airflow ratio decreases both the capacity of cooling and heating of the system. As well as, it is concentrated that the temperature performance of the refrigerator system is highly associated with the degree of free air accumulated by the accrued frost. The defrost studies identified the optimal sequence of events that must be used when conducting defrost cycles and considered the energy requirements of defrosting the industrial evaporator coils. It is approximated that 75%-85% of the energy necessary to defrost returned to the refrigeration system as additional load whereas the use of dampers during the defrosting helped to enhance the efficiency of the refrigeration system. Many studies mentioned the development of demand defrost controls as an alternative for timed defrost to avoid unneeded defrost and decrease the consumption of energy. In all of the preface studies on defrosting, the defrost process takes time and energy to melt the frost from the evaporator. Therefore, in this study, we endeavor to improve the defrost method, which in turn enhances the refrigeration system performance in cold storage rooms. In the next chapter, we discuss the installation of a simple cold storage room that works as normal with the electric heater defrost method and we investigate the effects of the defrosting process on cooling rooms and the temperature rises during defrost cycles. Then, we discuss how we applied the new defrost method and reported the changes on:

- the energy needed for the defrosting process;
- the defrosting efficiency;
- the refrigeration efficiency and COP; and
- the temperature fluctuations in the cooling room during the defrosting process.

PART 3

EXPERIMENTAL TEST FACILITY

This part presents a detailed description of the experimental test facilities used in this research, which consisted of an assembled cold storage room with its refrigeration system in addition to a data acquisition system. The units were used to test the system performance in terms of energy consumption, pressure, refrigerant weight, and temperature.

3.1. EXPERIMENTAL COLD STORAGE COMPARTMENT

As shown in Figure 3.1, the refrigerated compartment has been designed to represent the performance of a typical cold storage room compartment. The refrigeration system, with its height of 80 cm, width 60 cm, and length 120 cm, was designed to mimic the volume of the refrigerated compartment. Our study designed a refrigerated compartment with internal dimensions of 104 cm length, 44 cm width, and 64 cm height, and an internal volume of 0.292.8 m^3. The door, floor, walls, and ceiling of our refrigerated compartment were constructed from the same material, namely 80 mm thick high-density (40 kg/m^3) polyurethane foam panels with galvanized steel and a white PVC coating. The crevices between the ceiling panels, walls, and floor were sealed with a white silicone sealer to decrease the leakage of water into the panels. The refrigerated compartment was constructed on a mobile steel support framework to facilitate movement in the workshop and the mobile steel framework was designed with two levels. The first level was used to install the refrigeration component compressor, condenser, and other components, and the refrigerated compartment was installed on the second level, as shown in Figure 3.1. Two evaporators were installed in the backside of the refrigerated compartment facing the door.

Figure 3.1. The cold storage room compartment.

3.2. THE REFRIGERATION SYSTEM OF THE EXPERIMENTAL COLD ROOM

The refrigeration system comprises (1) a hermetic reciprocating compressor type Embraco model NEU6215GK; (2) a forced-air condenser type HTS with an ELCO fan motor; (3) a filter drier with welding terminals; (4) a two-meter long, 0.17 mm diameter capillary tube and used as an expansion device; (5) a four-way valve to change the refrigerant path between evaporators; (6) two evaporators air cooler type KARTER model EL-15AE5-C22 with R404a refrigerant fluid; (7) a superheat subcooling heat exchanger; and (8) copper pipes to connect between the system parts, a 6 mm discharge line, a 6 mm liquid line and a 10 mm suction line. More specifications of these components are shown in Table 3.1. The experimental cold

room components and the data acquisition instruments connected to the refrigeration system are shown in Figures 3.2 and 3.3.

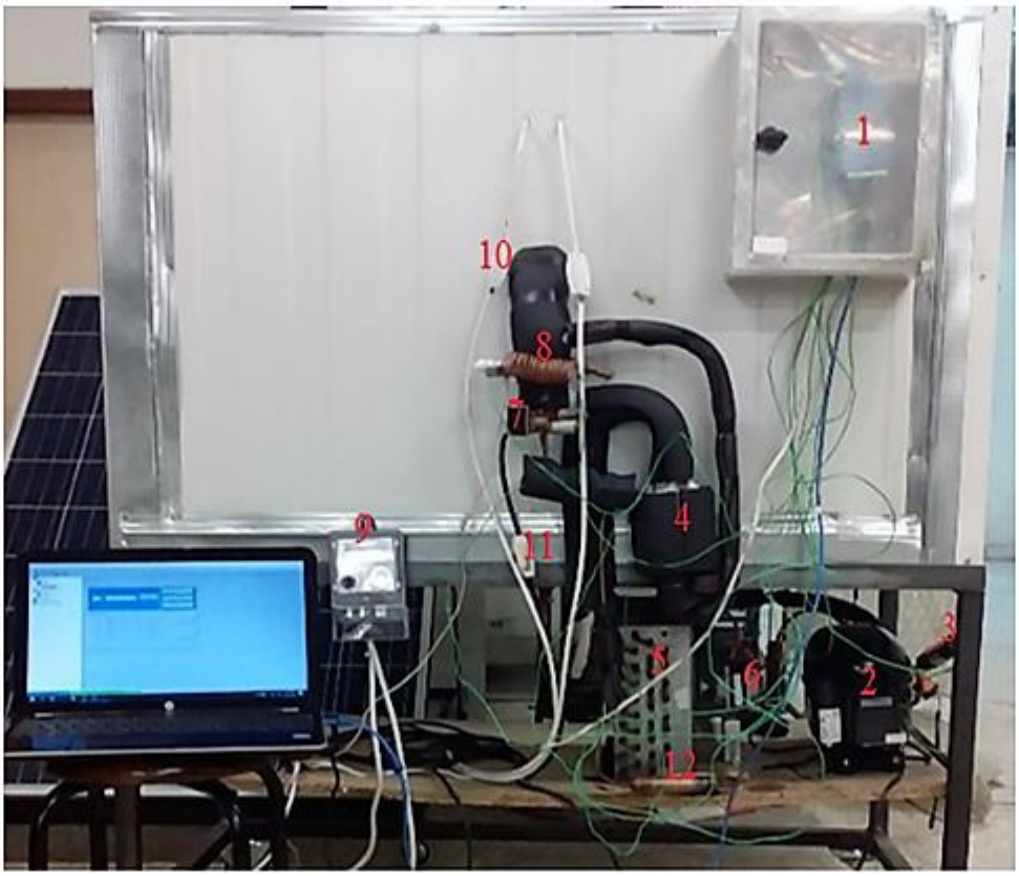

1- Temperature Recorder
2- Compressor
3- Pressure Test
4- Heat Exchanger
5- Condenser
6- Condenser Fan
7- Four-Way Valve
8- Capillary Tube
9- Power Test
10- Evaporator Fan Switch
11- Four-Way Valve Switch
12- Filter Drier

Figure 3.2. Refrigeration system components.

The temperatures were measured with K-type thermocouples with the ADAM model 4019 connected to a personal computer recording data every two seconds in eight points on the system. Four pressure points were measured using a TESTO 549i pressure sensor probe connected to an Android tablet recording pressure data every two seconds. The energy consumption of the system was measured with a Köhler wattmeter. Table 3.2 shows the details of the components.

Table 3.1. Characteristics of the main components of the system.

Components	Characteristics	Value
Compressor	Embraco NEU6215GK.	0.5 Hp
	High starting torque	HBP
	Displacement	12.11 cm^2
	Full load current	4.48 A
Condenser (HTS forced air condenser)	Type	Fin-tube
	ELCO Fan motors	65 W
	Current	0.45 A
Evaporators KARTER (EL-115AE5-C22)	Type	Fin-tube
	Fin spacing	5.5 mm
	Max/min temp	−45/50
	Capacity	355 W
	Volume	0.2 dm^3
	Airflow	205 m^3/h
	Total surface	1.2 m^2
	Energy efficiency class	C
	Pipe material	copper
	Fin material	aluminum
	One fan	23 W-0.1 A
	Electric heater	0.32 kW
	Dimension	50 cm × 39 cm × 8 cm
Refrigerant	404A	170 g
Expansion device	Capillary tube	
	Length	2 m
	Inside diameter	0.14 mm
Four-way valve	DHF-5	4 kW
Power supply	For all components	220 V/50 Hz

1- Evaporator Number 1
2- Evaporator Number 2
3- Evaporator Fan
4- Evaporator Inlets
5- Evaporator Outlets
6- Defrost Heaters
7- Derange Pan
8- Capillary Tube
9- Evaporator Fans Switches
10- Four-Way Valve Switch
11- Evaporators 1 Inlet Test Point
12- Evaporators 2 Inlet Test Point

Figure 3.3. Placing the evaporators inside the room with the four-way valve and capillary tube in the back of the room.

3.3. HEAT EXCHANGER

In order to improve refrigeration efficiency, a heat exchanger was designed for the system. Liquid line-suction line heat exchangers are usually used in refrigeration systems to ensure the correct cycle operation and to increase refrigeration system performance. ASHRAE (1998) stated that liquid line-suction line heat exchangers are efficient in many areas, such as the following [55]:

1. Increase in the performance of the system
2. The use of subcooling liquid refrigerant to avoid the accumulation of flash gas in the inlets of expansion devices
3. The complete evaporation of any residual liquids that may remain in the liquid suction before accessing the compressor

The heat exchanger used in this study is a liquid-suction heat exchanger, the schematic and photo of which are shown in Figure 3.4. The shell and tube heat exchange comprises of a circulated shell diameter of 8 cm and length of 12 cm, and tube of

length 104 cm and diameter 6 mm. The surface contact area between the liquid line and suction line is 195.9 cm^2.

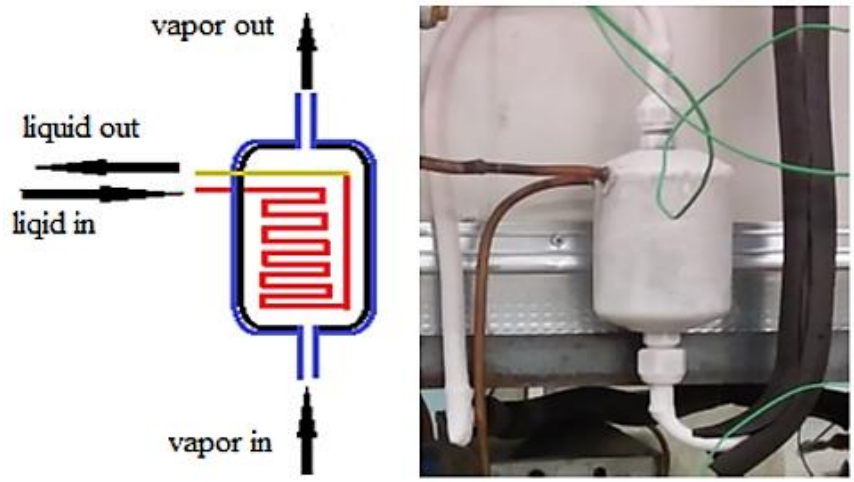

Figure 3.4. Liquid-suction heat exchangers.

3.4. REFRIGERANT SELECTION

The selection of a suitable refrigerant was made according to some physical properties, thermodynamic properties, and chemical properties. The refrigerant that satisfies all the required thermodynamic, physical, and chemical properties can be called the ideal refrigerant. However, different refrigerants may seem to satisfy all the requirements and sometimes only partially. A refrigerant that is suitable in a specific application may completely fail in other applications. Hence, the refrigerant has to be selected for this application in such a way that most of the basic properties should be favorable for the application. The most necessary properties of the refrigerant for this system should include a low boiling point which is suitable for cooling rooms (ca. −30°C) and a low freezing point because we have high subcooling in the liquid line refrigerant located in the refrigerated compartment. The other properties should be similar to any refrigerant, including high critical pressure and temperature points, non-flammability, high COP in the working temperature range, high thermal conductivity, ready availability and low cost, high miscibility with lubricating oil, and of course, the refrigerant should have minimal environmental effects relating to ozone layer depletion and global warming potential. According to its properties, R404a was

selected as a refrigerant fluid for the system. Figure 3.5 shows the unit charging with the refrigerant.

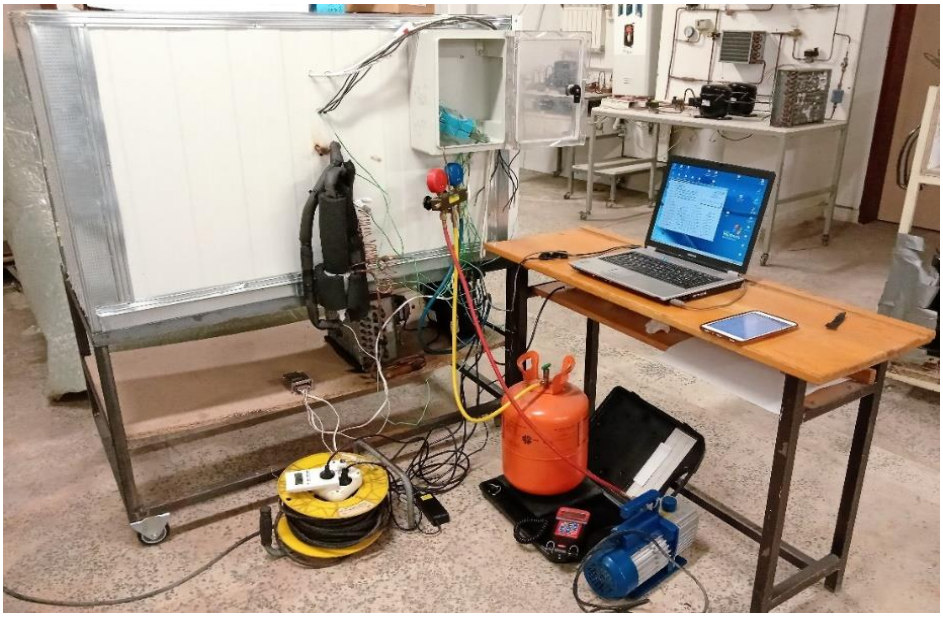

Figure 3.5. Charging the unit with R404a refrigerant.

3.5. DATA ACQUISITION SYSTEMS

When discussing data acquisition systems (usually abbreviated as DAS), we refer to the process of making measurements and recording any physical phenomena according to a method to analyze them. The collection of data is widely recognized as distinct from earlier ways of documentation, such as tape charts or paper charts. Unlike those approaches, the signals are transformed to the digital domain from the analog domain and then recorded to the digital medium, including a hard disk drive, ROM, or flash medium. Digital data acquisition systems used in this thesis included pressure measurement, temperature measurement, refrigerant mass measurement, and power measurement.

3.5.1. Pressure Probe Measurement

The Smart Probe Testo 549i was used to measure the pressure in this experiment. It is a hose-less, wireless device that measures the refrigerant pressure of the refrigeration

system (see Figure Appendix 1). It is commonly used to examine and record the operations of commercial and residential refrigeration systems. The measurements can be read by the operator with the Testo Smart Probes App installed on his smart device. The Testo 549i connects the standard Schrader valves without hoses and any other tools, thereby avoiding any loss of refrigerant. The Testo 549i operates on smart mobile phones such as Apple and Android operating systems at a distance of up to 9 meters. It is possible to read the measurements remotely from six Smart Probes simultaneously and report and record the results easily. All measurement data can be displayed as instrument graphs, readings, and tables. Moreover, the measurement data can be quickly stored in PDF and Excel files and can be saved and retrieved quickly, saving many hours of paperwork. The general data for the Testo 549i is presented in Table Appendix 1.

3.5.2. Temperature Data Logger

For temperature measurements, an ADAM Module 4019 with type K thermocouples was used to measure and record the temperature every two seconds for all measuring points on the system. The ADAM series are intelligent sensor-to-computer interface units and comprise an in-built microprocessor. A simple set of commands is used to control the ADAM series transferred following the RS-485 protocol and issued in ASCII format. The ADAM Module 4019 8-channel Universal Analog input units use a microprocessor-controlled integrated digital/analog converter to convert the current, thermocouple, sensor voltage, and signals into digital data. Later, the digital data are translated into engineering modules, twos-complement the hexadecimal format or percentages of Full-Scale Range (FSR) following the constitution of units. When demanded by the host computer, the data are transferred through a standard RS-485 interface. The Analog Input Modules provide RS-485 digital communication functions, Analog/Digital conversion, signal conditioning, and ranging. The measurement range and accuracy are shown in Table Appendix 2. The computer is connected to a single convertor type ADAM-4561 across the RS232 interface and transforms commands from the output units of the ADAM network, as shown in Figure Appendix 2. Every output comprises several electrical switching outputs. The type of

output unit determines the type and number of switching units. The output of the switching control signals or announces its status to other devices.

3.5.3. Refrigerant Charging Measurement

The digital programmable electronic charging scale RES-100, as shown in Figure 3.10, was used to measure the refrigerant mass of the system. The refrigerant scales were used not only when initially installing refrigeration systems but also during regular maintenance and repairs. As the refrigerant is removed from the compressor, the scale measures its weight. While troubleshooting to find leaks, the scale can be extremely useful for techs. An accurate reading is highly valuable as it ensures that the correct amount of refrigerant is being recovered or charged from the compressor. Its specifications are shown in Table Appendix A3. This helps to recharge accurately and keeps the system working at energy-efficient, optimal performance levels. Figure Appendix A3 shows a photo of the scale.

3.5.4. Power Consumption Measurement

The Köhler model AEL.MF.07 ampere active single-phase counter was used to measure the consumption of power by the refrigeration system during the testing phase. Table Appendix A4 enumerates the specifications of the instrument and Figure Appendix A4 shows a photo of the instrument.

PART 4

EXPERIMENTAL TEST PROCEDURE

This chapter describes the procedure of the experiment for the electric heater defrost method and the new defrost method. Moreover, details and analyses for refrigeration system performance during the cooling process and defrosting process for both methods are given.

4.1. EXPERIMENTAL PROCEDURE

The experiments were conducted at an ambient temperature of 19.3°C and compartment air temperature of −20°C. The experiments were carried out on the system in two states. In the first state, the system was connected as a normal cycle with one evaporator using an electric heater as a defrosting method. Figure 4.1 shows the refrigeration cycle of the system. The experiment lasted nine hours with four defrost cycles and recorded the measurement during the operation time. Then we reconnected the system according to the *New Defrost method* with two evaporators and a four-way valve. Figure 4.2 shows the refrigeration cycle form and its cycle on a log P-h diagram. Additionally, the new method experiment operated under the same conditions as the first state, for nine hours with four defrost cycles and recorded the measurement during the operation time. The defrost cycle was manually started in both methods. In the normal method (Electric Heater), the defrost process was started by operating the heater for 10 minutes until all the frost had melted; the interval between defrost cycles was two hours. In the New Method, the defrost process was started by switching on or off the four-way valve to change the refrigerant direction between the evaporators.

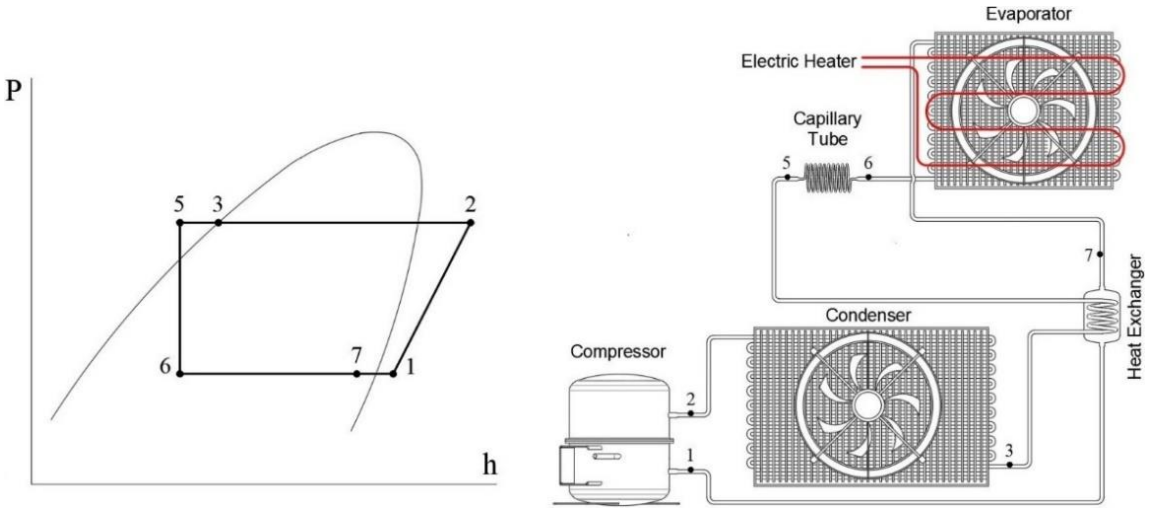

Figure 4.1. Refrigeration cycle on the log P-h diagram following the electric heater method.

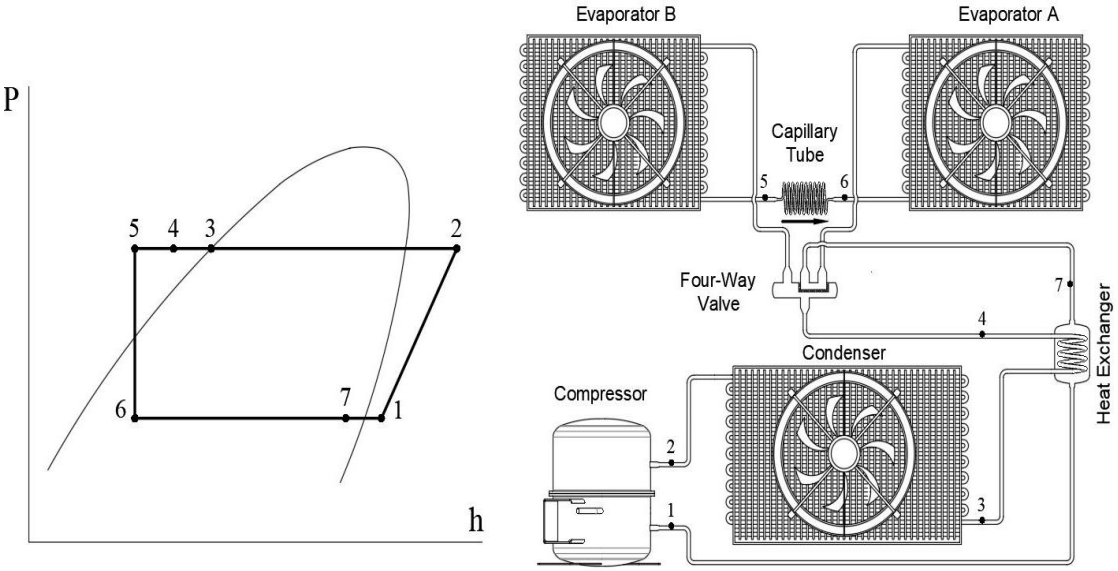

Figure 4.2. Refrigeration cycle on the log P-h diagram following the new method.

In this method, the system operated while the evaporator (A) fan was ON and the evaporator (B) fan and the four-way valve were OFF. Two hours later, the evaporator (B) fan and four-way valve switched ON and the evaporator (A) fan switched OFF in order to start the evaporator (A) defrosting process and evaporator (B) cooling process. Figures 4.3 and 4.4 show the refrigeration cycle when evaporators (A) and (B) are in the defrosting process and show the measurement point's Ⓣ for temperature and Ⓟ for pressure.

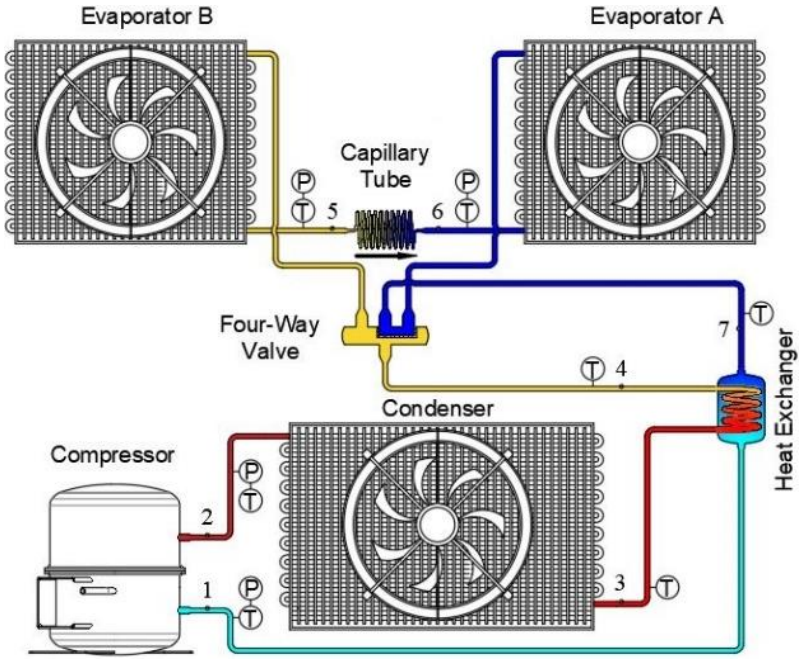

Figure 4.3. Schematic of the system when evaporator B is in the defrosting process and evaporator A is in the cooling process.

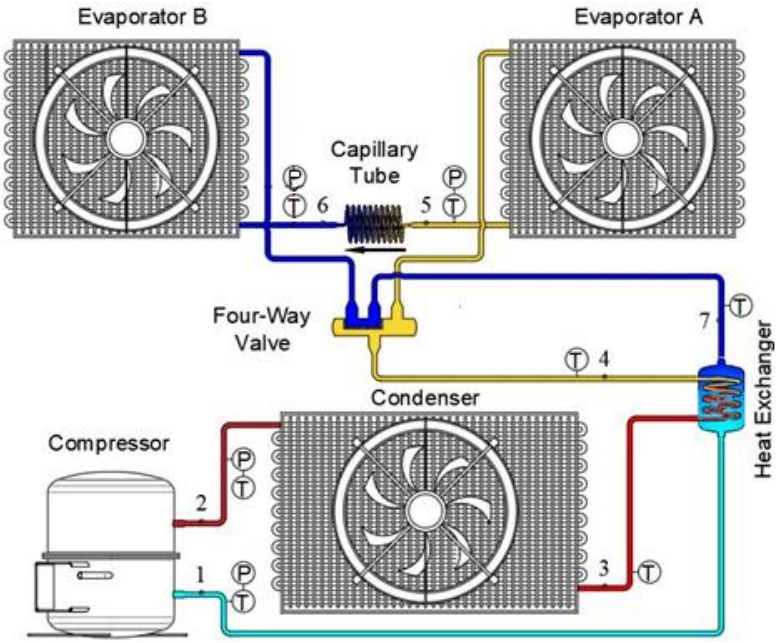

Figure 4.4. Schematic of the system when evaporator A is in the defrosting process and evaporator B is in the cooling process.

4.2. PLOTTING THE REFRIGERATION CYCLE ON A LOG P-h DIAGRAM

The cycle of refrigeration is expressed as a sequence of status changes of refrigeration system properties. The status variables in the refrigeration cycle, including density, temperature, and pressure, are significant due to the dependency of the variables' status on each other. The thermodynamic operations of the refrigeration system are complicated. Thus, with the use of a plot on the pressure/enthalpy diagram, the numerous status variables can be represented graphically according to their dependencies. It is possible to read the thermodynamic status variables directly in each status point and they are available for additional calculations. Pressure differences of status change, heat quantities, and technical works are presented as measurable lines. Plotting the refrigeration cycle on the thermal pressure diagram explains the thermodynamic calculations. It is important to understand the operating formula of the refrigeration cycle; therefore, the *cool pack* software for refrigeration equipment is used to display specific data on the log P-h diagram in real-time. Changes in operating parameters can be read directly from the diagram, thereby allowing important information such as the thermodynamic status to be presented, which otherwise can only be represented statically.

4.3. THEORETICAL ANALYSIS OF THE SYSTEM

The system performance analysis that was implemented is based on the First and Second Laws of Thermodynamics depending on the electrical and mechanical efficiency. The First Law of Thermodynamics is associated with energy conservation. Exergy does not resemble energy such that it is not subject to the conservation law of real systems [56]. Exergy analysis is concerned with the Second Law of Thermodynamics and is an important tool to design and optimize the performance of evaluation energy systems [57]. The main purpose of exergy and energy analyses is to identify the best performance of the systems and determine the locations of exergy destruction [58].

4.3.1. Energy Analysis

The main objective for the first law of thermodynamic analysis is to identify the variation of the coefficient of performance (COP) with the superheating temperature, condenser temperature, compressor isentropic effectiveness, and evaporator temperature. Therefore, the first law of thermodynamic analysis has been applied to every system element [58]. The refrigerant mass flow ratio (m_r) was calculated from the enthalpy at the points h_1, h_2, and the power of the compressor (P_{comp}) was calculated from the following two equations:

$$\dot{m}_r = \frac{\dot{W}_{comp}}{h_2 - h_1} \tag{4.1}$$

$$\dot{W}_{comp} = \dot{P}_{comp}\, \eta_{mec}\, \eta_{el} \tag{4.2}$$

The amount of heat transferred from the storage room to the evaporator for each unit time can be calculated with the following equation:

$$\dot{Q}_{ev} = m_r(h_7 - h_6) \tag{4.3}$$

The amount of heat that is transferred from the condenser to the evaporator for each unit time can be calculated by the following equation:

$$\dot{Q}_{con} = \dot{m}_r(h_2 - h_3) \tag{4.4}$$

The COP of the refrigeration system signifies the electrical power which is consumed by the compressor, which corresponds to the heat transferred from the evaporator for each unit of time. The COP can be calculated from the following equation:

$$COP = \frac{\dot{Q}_{ev}}{\dot{P}_{comp}} \tag{4.5}$$

The amount of heat that is transferred from the liquid refrigerant to defrost the frosted evaporator for each unit time can be calculated from the following equation:

$$\dot{Q}_{def} = \dot{m}_r(h_4 - h_5) \tag{4.6}$$

The effectivity of the heat exchanger that represents the rate of real heat transfer amount to the greatest heat transfer amount in the system is obtained thus:

$$\varepsilon_{hex} = \frac{T_{Li} - T_{Lo}}{T_{Li} - T_{So}} \tag{4.7}$$

4.3.2. Exergy Analysis of the System

The Second Law of Thermodynamics analysis depends on the exergy concept. Exergy is imagined as a measure of quality or possibility of work for different procedures of energy associated with environmental circumstances. Its analysis, which is applied to the system, describes all losses in the system elements [59]. This enhancement can help to understand the potential of these losses or irreversibility and their order of significance. Irreversibility is a measure of process deficiency and helps to determine the optimal operating circumstances. It can be said that an exergy analysis may refer to the possibility of increasing the thermodynamic enhancement of the process under consideration [60]. Moreover, it is possible to say that the exergy analysis is considered a new method in which energy loss evaluation follows from the Second Law instead of the First Law of Thermodynamics. Therefore, this analysis is related to the Second Law of Thermodynamics analyses [61]. The general exergy balance can be expressed in the rating form [62]. Therefore, exergy analysis was performed in this research. The exergy destruction for a continuous flow control volume is expressed as Equation 4.8 [63]:

$$\dot{E}_{x,dest} = \sum \dot{E}_{x,in} - \sum \dot{E}_{x,out} + \sum \left[\dot{Q}\left(1 - \frac{T_o}{T}\right)\right]_{in} - \sum \left[\dot{Q}\left(1 - \frac{T_o}{T}\right)\right]_{out} + \sum \dot{W}_{in} - \sum \dot{W}_{out} \tag{4.8}$$

The exergy destruction of the system is calculated using Equation 4.8. The first two items on the right side of Equation 4.8 represent the flow exergy. The next two items

represent the heat transfer energy and the last two items represent the work exergy. The sub-indices 'out' and 'in' in all of the equations in this study represent the outlet and inlet conditions. The ambient temperature was measured as a reference temperature (T_o).

The flow exergy to each point of the system is calculated as follows:

$$\dot{E}_x = \dot{m}_r[h - h_o - T_o(S - S_o)] \tag{5.9}$$

The analyzed system consists of a heat exchanger, condenser, compressor, capillary tube, and evaporator. Equations 4.10 and 4.11 were used to calculate the exergy destruction for each item of the system exergy analysis, thus:

$$\dot{E}_{x,dest,comp} = \dot{E}_{x,1} - \dot{E}_{x,2} + P_{comp} \tag{4.10}$$

$$\dot{E}_{x,dest,comp} = \dot{m}_r[(h_1 - T_oS_1) - (h_2 - T_oS_2)] + P_c \tag{4.11}$$

The general expression of the exergy destruction is calculated with Equations 4.12 and 4.13:

$$\dot{E}_{x,dest,con} = \dot{E}_{x,2} - \dot{E}_{x,3} - \left[\dot{Q}_{con}\left(1 - \frac{T_o}{T_{con}}\right)\right] \tag{4.12}$$

$$\dot{E}_{x,dest,con} = \dot{m}_r[(h_2 - T_oS_2) - (h_3 - T_oS_3)] - \left[\dot{Q}_{con}\left(1 - \frac{T_o}{T_{con}}\right)\right] \tag{4.13}$$

Equations 4.14 and 4.15 were used to calculate the exergy destruction of the system evaporator:

$$\dot{E}_{x,dest,ev} = \dot{E}_{x,6} - \dot{E}_{x,7} + \left[\dot{Q}_{ev}\left(1 - \frac{T_o}{T_{ev}}\right)\right] \tag{4.14}$$

$$\dot{E}_{x,dest,ev} = \dot{m}_r[(h_6 - T_oS_6) - (h_7 - T_oS_7)] + \left[\dot{Q}_{ev}\left(1 - \frac{T_o}{T_{ev}}\right)\right] \tag{4.15}$$

Equations 4.16 and 4.17 were used to calculate the exergy destruction of the capillary tube:

$$\dot{E}_{x,dest,cap} = \dot{E}_{x,5} - \dot{E}_{x,6} \tag{4.16}$$

$$\dot{E}_{x,dest,cap} = \dot{m}_r T_o (S_5 - S_6) \tag{4.17}$$

Equations 4.18 and 4.19 were used to calculate the exergy destruction of the heat transfer:

$$\dot{E}_{x,dest,hex} = \left(\dot{E}_{x,3} - \dot{E}_{x,4}\right) + \left(\dot{E}_{x,7} - \dot{E}_{x,1}\right) \tag{4.18}$$

$$\begin{aligned} \dot{E}_{x,dest,hex} = \dot{m}_r [\{(h_3 - T_o S_3) - (h_4 - T_o S_4)\} \\ + \{(h_7 - T_o S_7) - (h_1 - T_o S_1)\}] \end{aligned} \tag{4.19}$$

Equation 4.20 was used to calculate the total exergy destruction caused by the system components by adding each component thus:

$$\dot{E}_{x,dest,all} = \dot{E}_{x,dest,comp} + \dot{E}_{x,dest,con} + \dot{E}_{x,dest,ev} + \dot{E}_{x,dest,cap} + \dot{E}_{x,dest,hex} \tag{4.20}$$

Equation 4.21 was used to calculate the general exergy efficiency of the system as:

$$\eta_{gen} = \frac{\dot{E}_{x,6} - \dot{E}_{x,7}}{\dot{P}_{comp}} \tag{4.21}$$

4.3.3. Defrost Efficiency

Defrosting efficiency can be defined as the ratio of necessary defrosting heat energy to the heat energy released by a defrosting method [40, 59, 60], as shown in Equations 4.22, 4.23, and 4.24:

$$\eta_{def} = \frac{\dot{Q}_{melt}}{\dot{Q}_{def}} = 100\% \tag{4.22}$$

$$\dot{Q}_{melt} = \dot{m}_f \times f_i \tag{4.23}$$

$$\dot{Q}_{def} = \dot{Q}_{melt} + \dot{Q}_{losses} = \dot{P}_{def} \times t_{def} \quad (4.24)$$

where η_{def} is the defrosting efficiency, $\dot{Q}_{melt}$ the heat absorbed by the frost, $\dot{Q}_{def}$ the heat released by the defrosting device, $\dot{Q}_{losses}$ the heat lost by the defrost device in the refrigerator, m_f the mass of the frost melted through the defrosting process (kg), f_i the latent heat of frost liquefaction (334 kJ/kg), P_{def} the consumption of power by the defrosting device by (W), and t_{def} the time of defrosting process (seconds). In the new method, the entire defrosting heat flows from the subcooling heat in the liquid line. $Q_{def} = m_R(h_4 - h_5)$ and the defrosting process rises at the same time as the cooling process.

4.3.4. Thermodynamic Analysis of the System in the New Method

The systems start in a specific mode where evaporator A is in the cooling mode and evaporator B is in the defrosting mode. After a period of activating the four-way valve to defrost evaporator A, its temperature was approximately −28°C and becomes the liquid refrigerant line. Evaporator A body and frost will take the temperature from the liquid refrigerant. The liquid refrigerant sub-cooling begins at approximately 48°C and reduces gradually until all the frost melts. The sub-cooling during the defrosting phase is shown in Figure 5.4. The sub-cooling of the liquid refrigerant in the system is separated into two parts: heat exchanger subcooling (SC_{exh}), which occurs in the heat exchanger due to the superheat in the suction line, and defrosting subcooling (SC_{def}) occurs in the defrosted evaporator due to melting frost and heat losses in the storage room, as shown in Figure 4.5.

$$\dot{Q}_{def} = \dot{m}_r\,(h_4 - h_5) = \dot{Q}_{melt} + \dot{Q}_{losses} = SC_{def} \quad (4.25)$$

$$SC_{exh} = \dot{m}_r\,(h_3 - h_4)\ and\ SC_{def} = \dot{m}_r(h_4 - h_5) \quad (4.26)$$

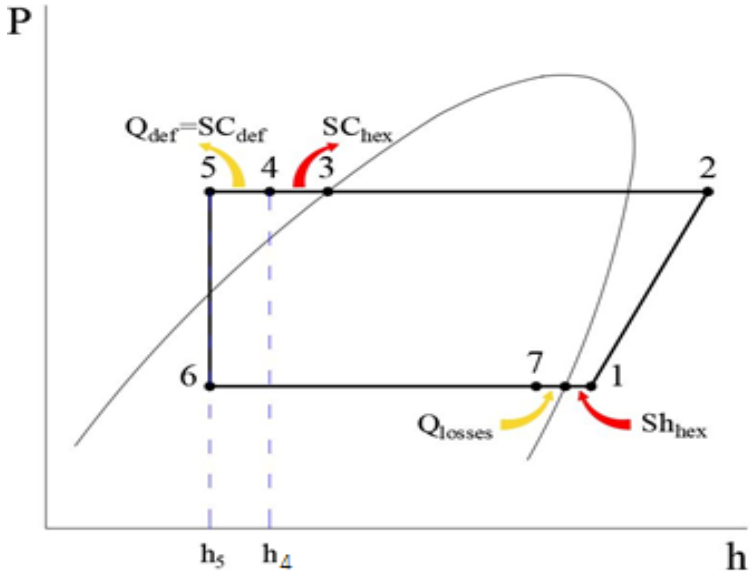

Figure 4.5. Inlet and outlet energy for the new method.

4.3.5. Economic-Environmental Analysis of the System

In this study, the cost of 1 kW of the cooling capacity (Q_E) is calculated by performing an economic analysis of both methods. Many elements must be taken into consideration, including annual maintenance cost (AMC), annual salvage value (ASV), capital recovery factor (CRF), sinking fund factor (SFF), and annual electric cost (AEC) in addition to the capital cost (P). The CRF here can be defined as a function of the annual interest rate (i) and life of the system (n) [61,62]:

$$CRF = \frac{i(1+i)^n}{(1+i)^n - 1} \tag{4.27}$$

It is assumed that the life in years of the system (n) and the annual interest rate (i) are 20 years and 12%, respectively [61, 62]. Then, the fixed annual cost (FAC) can be calculated as follows:

$$FAC = P(CRF) \tag{4.28}$$

where P is the cost of materials used, including condensers, evaporators, sandwich panels, compressors, fans, and other components. The salvage value (S) is calculated thus [61]:

$$S = 0.2P \tag{4.29}$$

Equations 4.30 and 4.31 respectively calculate the SFF and ASV as follows:

$$SFF = \frac{i}{(1+i)^n - 1} \tag{4.30}$$

$$ASV = (SFF)S \tag{4.31}$$

The AMC of the system may include the addition of annual maintenance, calculated thus:

$$AMC = 0.15(FAC) \tag{4.32}$$

Equations4.33 and 4.34 calculate the annual power consumption (APC) and annual electric cost (AEC) as follows:

The Annual power consumption of the refrigeration system with the electric heater defrost method is calculated thus:

$$APC_{E.H} = \dot{P}_c\, t_c + \dot{P}_d\, t_d \tag{4.33}$$

The annual power consumption of the refrigeration system with the new defrost method is calculated thus:

$$APC_{new} = \dot{P}_c\, t_c \tag{4.34}$$

where $APC_{E.H}$ and APC_{new} are the annual power consumption of the refrigeration system with the electric heater method and with the new defrost method, respectively.

P_c is the compressor power, t_c is the annual use time, and P_d and t_d are the heater power and heater annual use time, respectively.

$$AEC = (APC)\Omega \tag{4.35}$$

where, Ω is the price of 1 kWh of electricity. The annual cost (AC) is calculated thus:

$$AC = FAC + AEC + AMC - ASV \tag{4.36}$$

Thus, the annual cost of 1 kW of cooling capacity is calculated thus:

$$CPC = \frac{AC}{COP} \tag{4.37}$$

where COP is the performance coefficient of the refrigeration system.

The enviro-economic analysis is implemented by taking the carbon emissions cost, which is approximately 2 kg per kWh of energy. The annual CO_2 emissions of the system (ϕ_{CO_2}) is calculated thus [63]:

$$\phi_{CO_2} = \Psi_{CO_2} \times (APC) \tag{4.38}$$

where Ψ_{CO_2} is the mean of CO_2 emission (2 kgCO_2/kWh) when coal is used to generate electricity. The international price of carbon (z_{CO_2}) is \$14.5/tonCO_2. The environmental cost (Z_{CO_2}) is derived from the following equation:

$$Z_{CO_2} = z_{CO_2} \times \phi_{CO_2} \tag{4.39}$$

4.4 ERROR ANALYSIS

In this study, the effect of the uncertainties of the devices used in the experimental process on exergy and energy analyses was investigated using the equation below. This

equation is known as the Gaussian error propagation law. According to this law, *R* is a function such that *R* = *f*(*x*1, *x*2,… *xn*), and the error analysis of *R* is as follows [64]:

$$w_R = \left[+ \left(\frac{\partial R}{\partial x1} w_1 \right)^2 + \left(\frac{\partial R}{\partial x2} w_2 \right)^2 + \cdots + \left(\frac{\partial R}{\partial xn} w_n \right)^2 \right]^{1/2} \quad (4.40)$$

where, w_n is uncertainty in the n^{th} independent variable.

PART 5

RESULTS AND DISCUSSION

5.1. EXPERIMENTAL RESULTS

When the experiments were carried out, the ambient temperature was found to be 19.3℃ and the cold storage room temperature was −20℃ ± 2℃. The system was operated for approximately ten hours for both methods and the temperature, pressure, and power consumption values of the system for both methods were recorded. The experiment was conducted on the system using the new defrosting method for ten hours with defrosting occurring every two hours. Then, the electric heater defrosting method was performed under the same conditions. Figure 5.1 shows that the high and low pressures that continue throughout the working period of the system were equal, while in the electric heater method, the pressures were intermittent several times every two hours, which was caused by stopping the compressor for defrosting in the electric heater method.

In the new method, the compressor continues working until the system reaches the set point. The pressures in the system when using the new defrost method are more regular and stable in comparison to the electric heater method. When the compressor starts running, it draws a high current, and this is clear in the diagram in Figure 5.2 after each defrosting process. In the new method, there is a rise in current which results in switching the four-way valve to change the defrost process between the evaporators and it is less than the compressor starting current, as shown in Figure 5.2. The system in the new method consumes less power than the electric heater method and has a higher capacity, which means higher efficiency. The experimental results of the new defrost method show that the defrosting role of evaporator A is the same as evaporator B. Therefore, the defrosting of evaporator A and the cooling of evaporator B, have been analyzed in this study.

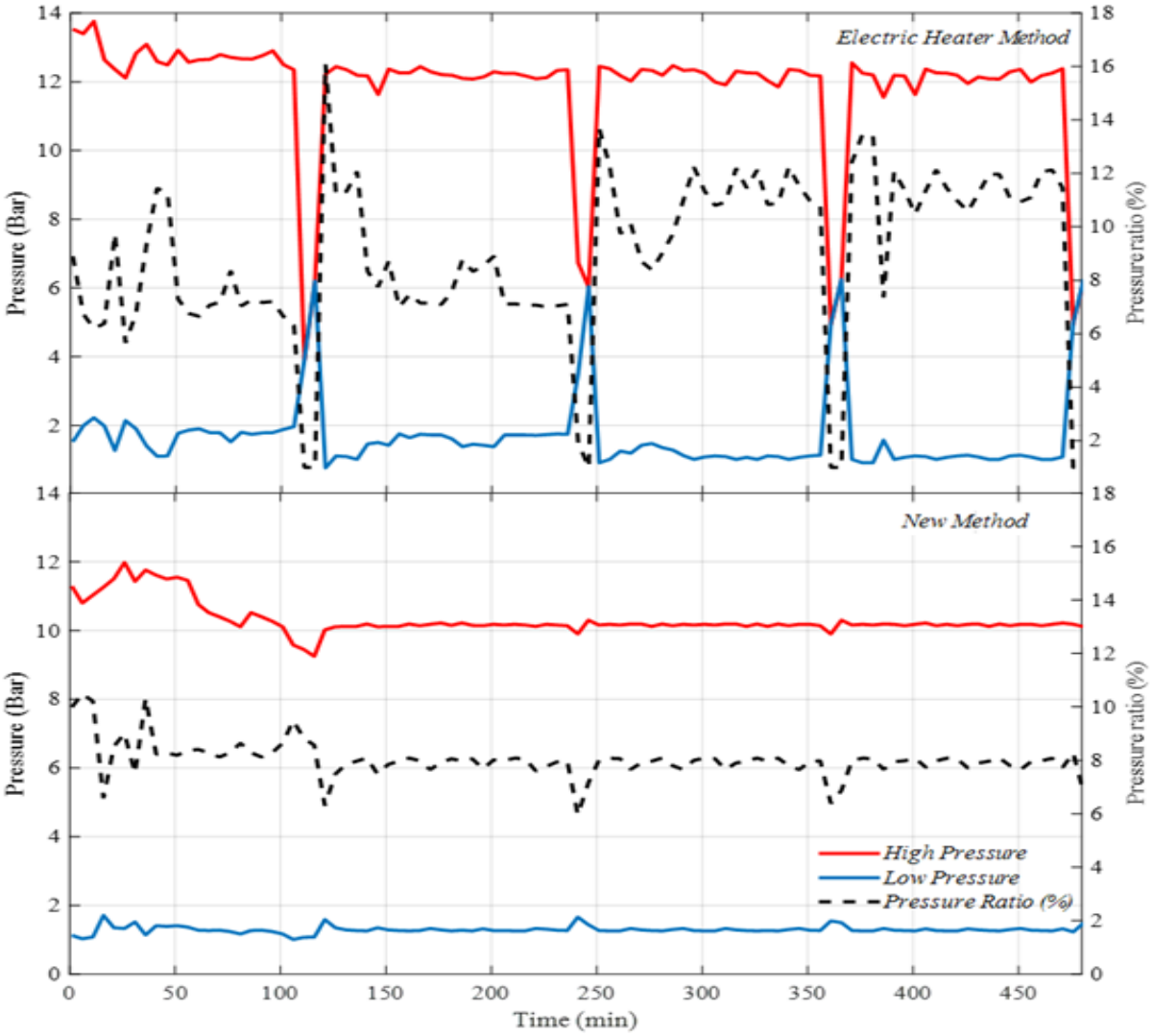

Figure 5.1. Changes in pressure ratios and high, low pressures for both methods.

When the four-way valve is switched to change the flow direction of the refrigerant between the evaporators to start defrosting evaporator A, the frost absorbs heat from the refrigerant liquid line. A high-pressure reduction and increase in liquid refrigerant sub-cooling occurs for some time (this depends on the amount of frost on the evaporator) and then returns to the normal state gradually.

Figure 5.3 shows the changes in high pressure and low pressure when the cooling process is switched between the evaporators. When the four-way valve is opened to change the cooling process between the evaporators, initially the low pressure rises sharply for about ten seconds; then it returns to the normal state, and the high-pressure decreases for about two minutes, after which it gradually returns to the normal state.

The storage room temperature in the middle of the evaporators 15 cm above the floor was measured.

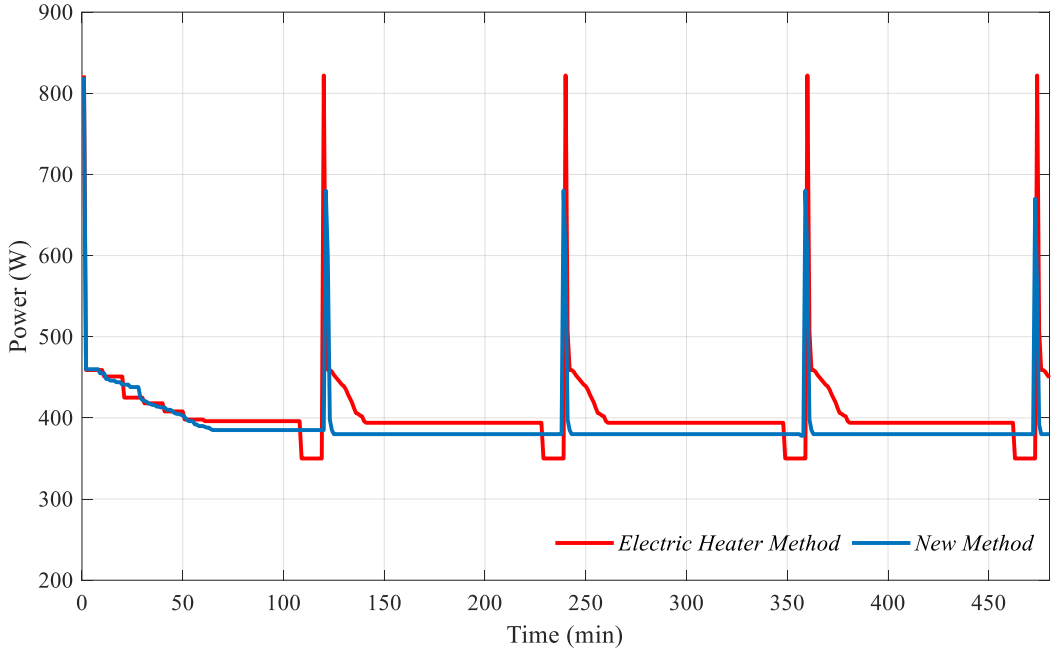

Figure 5.2. System power consumption for both methods.

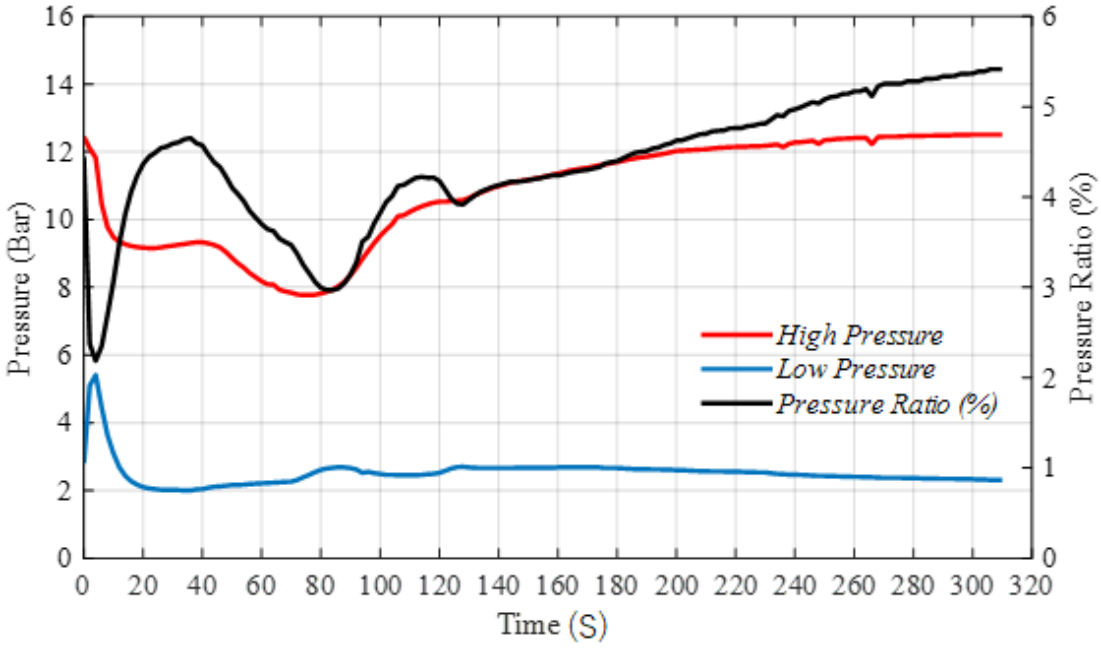

Figure 5.3. Pressure and compression ratio changes when changing defrosts between evaporators.

The temperature fluctuations in the compartment during the defrost process were approximately 14.5℃ in the Electric Heater Defrost Method. This rising in temperature is due to heat loss from the heater to the compartment. The temperature fluctuations were approximately 4.5℃ in the New Defrost Method, as shown in Figure 5.4. A large amount of heat loss occurred in the electric heater method because in the new method the defrost heat would occur at the same place where frost accumulated (i.e., in the pipe). However, in the electric heater, heat is generated in the heater and transferred to fins rather than to the pipe; therefore, a large portion of the heat radiates into the air.

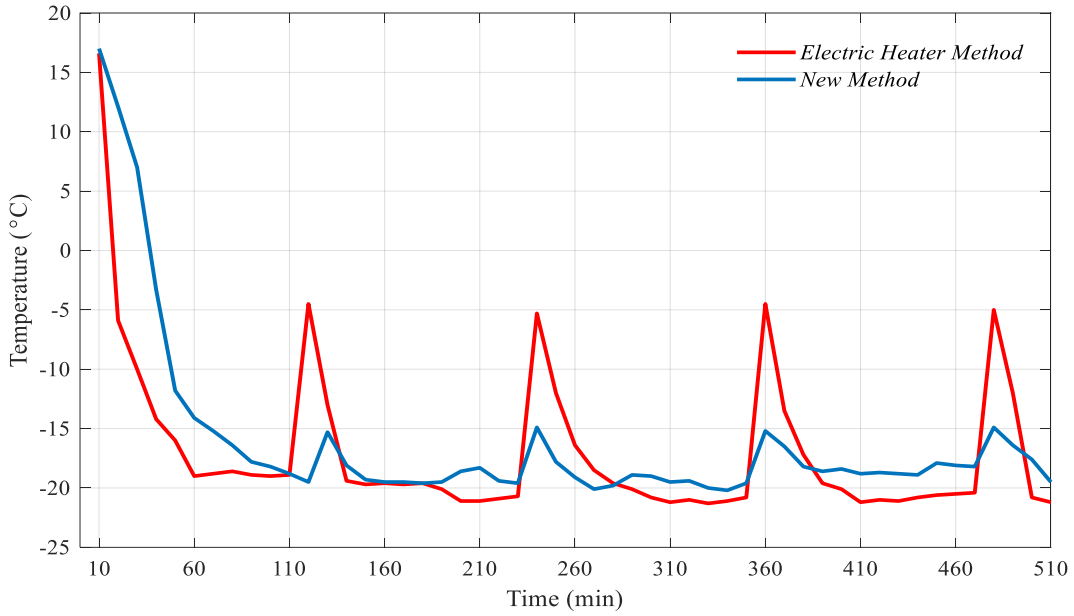

Figure 5.4. Storage room temperature changes during system working for both methods.

5.2. ENERGY EXERGY ANALYSIS RESULT

After plotting the refrigeration cycle for both methods on the pressure/enthalpy diagram, as shown in Figure 5.5, the numerous status variables were represented graphically according to their respective dependencies. It is possible to read the thermodynamic status variables directly at each status point and they are available for additional calculations. Pressure differences of status change, heat quantities, or technical work, are presented as measurable lines. The refrigeration cycle is colored red for the electric heater method and blue for the new method. The improvement of

the new method is visible in the log P-h diagram with its increases in sub-cooling, and reduction of compressor work this means a greater cooling effect and less energy consumption in the compressor.

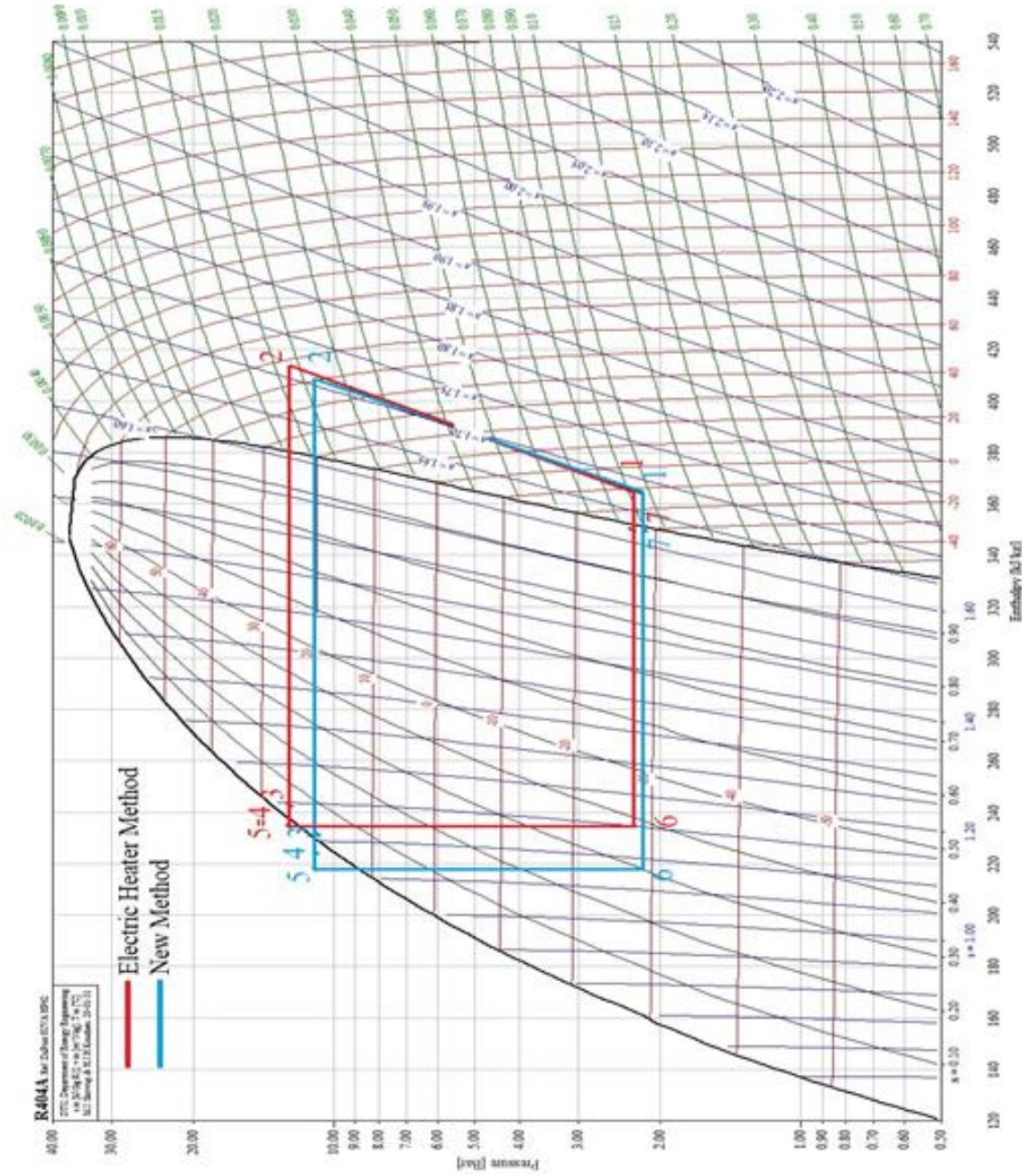

Figure 5.5. Refrigeration cycle on the log P-h diagram for both methods.

The thermodynamic parameters of the refrigeration cycle for the electric heater and the new methods recorded from the experiment are listed in Table 5.1. The pressure ratio in the electric method is higher than in the new method which causes higher

energy consumption in the compressor. The condensing temperature in the new method is lower than in the electric heater method due to heat loss in the defrosted evaporator. Low pressure and evaporating temperature are approximately the same and a little higher in the electric method. The specific enthalpy and specific entropy registered from the log P-h diagram for both methods are listed in Tables 5.2 and 5.3.

Table 5.1. Parameters measured from the system following both methods.

Item	Parameters (Unit)	New method	E.H method
L_P	Low pressure (bar)	2.26	2.41
H_P	High pressure (bar)	11.15	12.70
T_1	Suction line temperature (°C)	−12.8	−11.5
T_2	Discharge line temperature (°C)	51.1	57.5
T_3	Condenser outlet temperature (°C)	20.5	25.1
T_4	Heat exchanger outlet (sub-cooling)	19.2	23.5
T_5	Expansion device inlet temperature (°C)	12.5	23.5
T_6	Expansion device outlet temperature (°C)	−28.5	−27.3
T_7	Evaporator outlet temperature (°C)	−28.8	−27.5
T_R	Storage room temperature (°C)	−20	−20
T_a	Ambient temperature (°C)	19.3	19.3

Table 5.2. Parameters from the log P-h diagram for the electric heater method.

No	Parameters	Temperature (°C)	Specific enthalpy (kJ/kg)	Specific entropy (kJ/kg.K)
1	Compressor inlet	−11.5	364.6	1.683
2	Compressor outlet	57.5	414.3	1.717
3	Condenser outlet	25.1	241.5	1.143
4	Heat ex. outlet (SC)	23.5	235.4	1.121
5	Capillary tube inlet	23.5	235.4	1.121
6	Evaporator inlet	−27.3	235.09	1.152
7	Evaporator outlet	−27.5	350.4	1.624

Table 5.3. Parameters from the log P-h diagram for the new method.

No	Parameters	Temperature (°C)	Enthalpy (kJ/kg)	Entropy (kJ/kg.K)
1	Compressor inlet	−12.8	384.5	1.79
2	Compressor outlet	51.1	408.9	1.709
3	Condenser outlet	20.5	231.3	1.109
4	Heat ex. outlet (subcooling)	19.2	227.8	1.097
5	Capillary tube inlet	12.5	217.9	1.063
6	Evaporator inlet	−28.5	217.9	1.083
7	Evaporator outlet	−28.8	348.6	1.620

Parameters such as condenser load, evaporator load, coefficient of performance, compressor work, mass flow rate, and heat exchanger effectiveness were calculated according to the equations in Part 4 for both methods. The result shows that the mass flow rate in the new method was 7.03 g/s while in the electric method, it was 6.62 g/s in the same compressor with the same value metric displacement, which is due to higher refrigerant density entering the compressor in the new method. The compressor work (W) in the electric method is higher than in the new method, while the cooling effect is higher in the new method, resulting in higher COP and efficiency in the new method. The details of the thermodynamic analysis are listed in Table 5.4. for both methods.

Table 5.4. Details of the thermodynamic analysis of the system in both methods.

Symbol	Parameters (unit)	Electric Method	New Method
$\mathbf{Q_C}$	Condenser load (W)	1169.1	1256
$\mathbf{Q_E}$	Evaporator load (W)	764.6	849.9
COP	Coefficient of performance	1.94	2.23
$\mathbf{P_{COMP.}}$	Compressor power (W)	394	380
$\mathbf{m_r}$	Mass flow rate (g/s)	6.62	7.03
$\boldsymbol{\varepsilon_{hex}}$	Heat exchanger effectiveness (%)	18.5	18.5
$\boldsymbol{\eta_{is}}$	Isentropic efficiency (%)	75	79
$\boldsymbol{\eta_{el}}$	Electrical efficiency (%)	98	98
$\boldsymbol{\eta_{mec}}$	Mechanical efficiency of the compressor (%)	85	85

The exergy distractions analysis in Table 5.5 showed that the exergy destruction in the refrigeration system which used the electric heater method was found to be higher than the system that used the new method. Therefore, the new method is concluded to be more efficient in comparison to the system that uses the electric heater method. The exergy distraction ratio in the system parts was graphically drawn as in Figures 5.6 and 5.7, which is the increase in exergy destruction in the electric heater method in the compressor and the capillary tube. This increment is due to the increase in the pressure ratio in the electric heater method, while the other components, such as the evaporator, condenser, and heat exchanger, were the same.

Table 5.5. Details of exergy destruction analysis for both methods.

Parameters (Unit)	Electric Heater Method	New Method
Compressor exergy destruction (W)	139.1	123.2
Condenser exergy destruction (W)	12.4	12.7
Heat exchanger exergy destruction (W)	13.4	14.27
Capillary tube exergy destruction (W)	59.7	41.1
Evaporator exergy destruction (W)	21.6	16.2
Total exergy destruction (W)	246.2	207.5
Exergy efficiency (%)	36.1	47.9

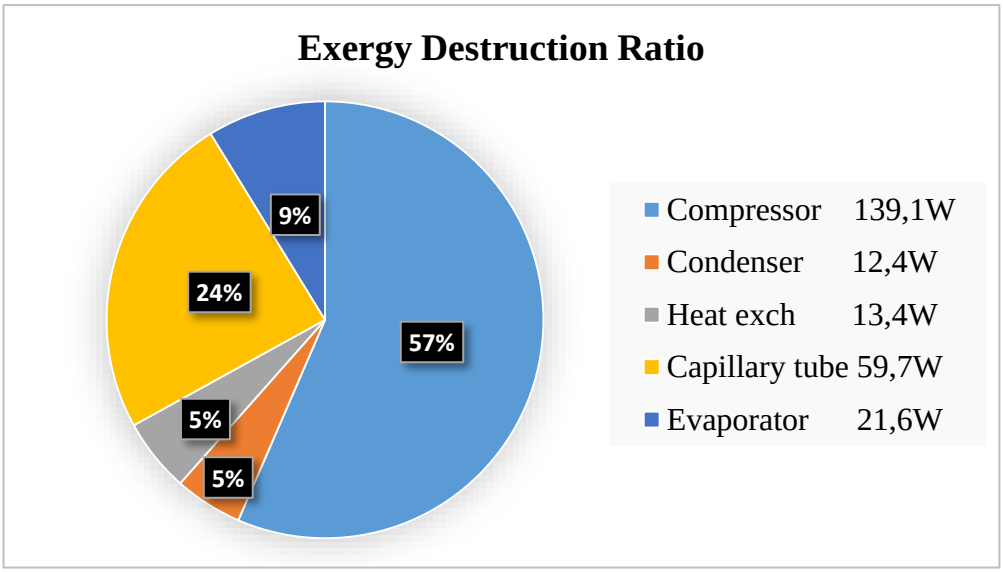

Figure 5.6. Exergy destruction ratio in the system with the electric heater method.

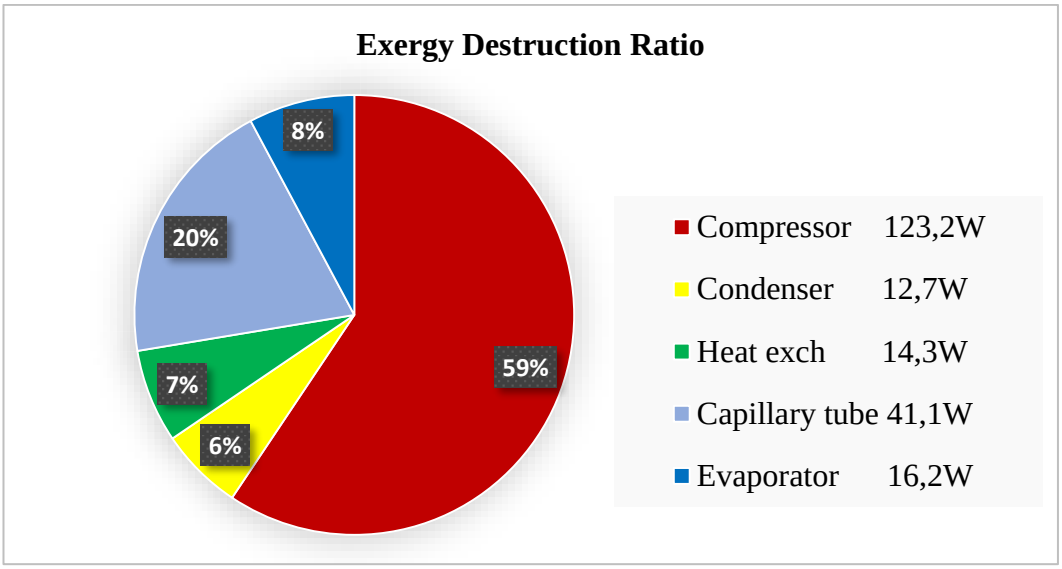

Figure 5.7. Exergy destruction ratio in the system with the new defrost method.

5.3. DEFROSTING EFFICIENCY RESULTS

The defrosting process was performed for both methods. Figure 5.8 shows images for the evaporator in the new method. Image (A) shows the frost accumulated on the evaporator before defrosting. Image (B) shows the evaporator after defrosting. Figure 5.9 shows infrared images for the temperature distribution in the evaporator and cold storage room during the defrosting process. The defrosting efficiency was calculated for both methods. In the electric heater method, the power consumed by the defrosting heater was 350 W, the mass of the melting frost was 89 g, and the time duration for the defrost cycle was 10 minutes; therefore, the defrosting efficiency was 15.5%, as shown in Table 5.8. In the new method, the entire defrosting heat flows from the sub-cooling heat in the liquid line. Figure 5.10 shows the amount of sub-cooling when the defrosting process started, starting at more than 50°C and decreasing gradually, thus resulting from the absorbed amount of heat by the liquid refrigerant in the defrosted evaporator. After all the frost melts, sub-cooling decreases to 17°C, as shown in Figure 5.10. The defrosting process occurs at the same time as the cooling process because there is no additional time or further energy for the defrosting process. Therefore, the defrosting efficiency can be considered to be 100% in the new method in the same systems as the electric heat defrosting method.

Table 5.6. Results of the electric heater defrost method.

Parameters	Definition	Value
P_{def}	Power consumed by defrosting device	0.350 kW
f_i	Latent heat of frost liquefaction	334 kJ/kg
m_f	Mass of melting the frost	0.089 kg
t_{def}	Defrost process duration	10 min
n_{def}	Defrosting efficiency	15.5%

Figure 5.8. Evaporator (a) before defrosting and (b) after defrosting.

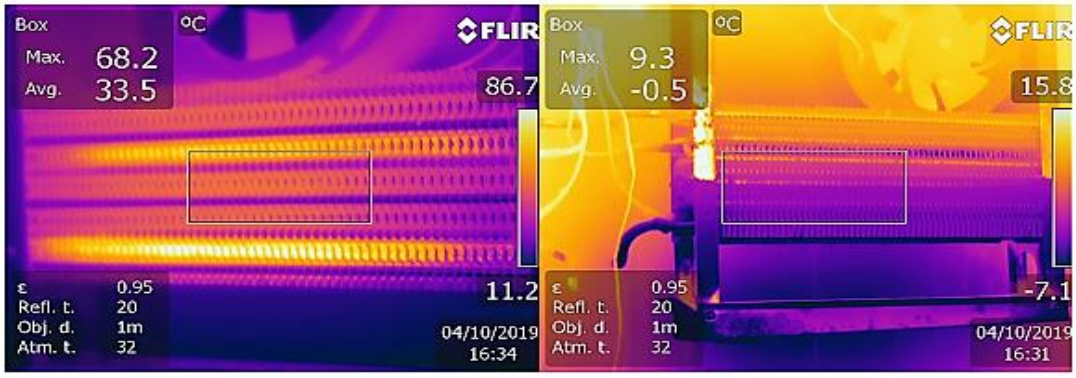

Figure 5.9. Infrared images showing the temperature distribution in the evaporator and cold storage room during the defrosting process.

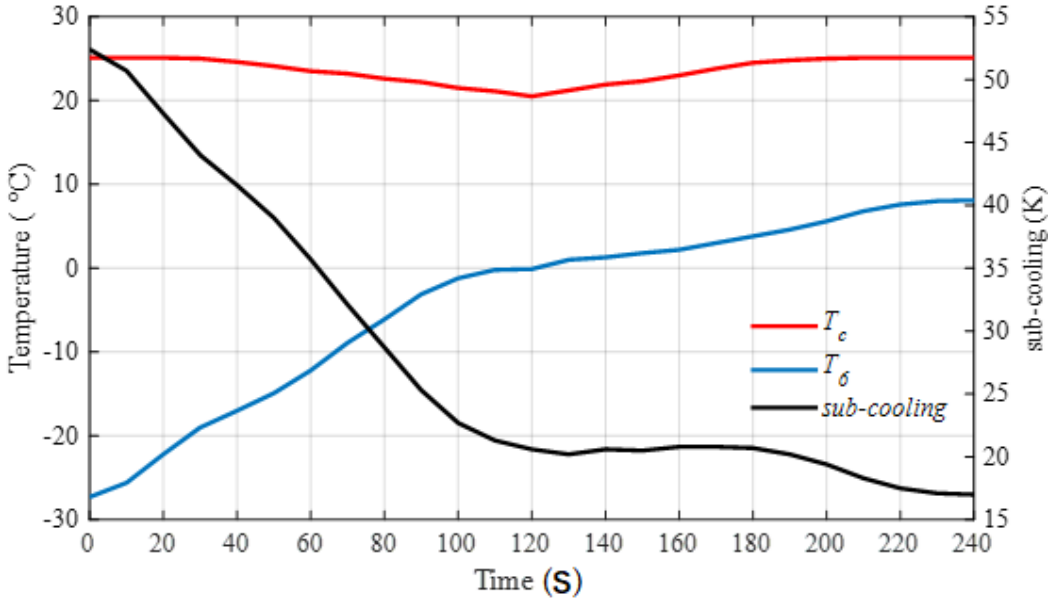

Figure 5.10. Sub-cooling (Tc-T6) during the defrosting process.

5.4. ENVIRONMENTAL-ECONOMIC ANALYSIS RESULTS

The environmental-economic analysis was conducted with details of the results listed in Table 5.6. The results show that the use of the new defrosting method system brought significant environmental-economic changes in the refrigeration system. The changes include an enhancement of the refrigeration system performance with the new defrost method being 12% better than the electric heater method in the same system. The cost of 1 kW of the cooling capacity (Q_E) decreased by 20% (from \$182.00 to \$147.10), but the costs of the system increased by 10% (from \$563 to \$618). Although the initial installation cost of the new method is \$55 more than the electric heater method, the annual power consumption (APC) is 11% lower (from 2763.7 kWh to 2469.6 kWh), and the annual electric cost (AEC) is 10% lower (from 259.7 to 234.6). This shows that the new method can recover its cost in a short time. The annual CO_2 emission amount is 10.7% lower (5.527 tonCO_2/year to 4.993 tonCO_2/year). The new method appears to be more environmentally friendly than the electric heater method. A comparison between both methods is listed in Table 5.7.

Table 5.7. Results of enviro-economic analysis of the study.

Parameter	Value	Unit	Parameter	Value	Unit
N	15	$	AMC	12.412	$
I	12	%	APCE.H	2763.7	kWh
t_C	6570	h	APCnew	2496.6	kWh
td	547.5	h	AECE.H	259.7	$
Pd	320	W	AECnew	234.6	$
P	740	$	CPCE.H	182.4	$
PC	394	W	CPCnew	147.1	$
Ω	0.094	$/kWh	ΨCO_2	2	$kgCO_2/kWh$
CRF	0.1339		E_{CO_2} new	4.993	$tonCO_2$/year
FAC	82.75	$	E_{CO_2} E.H	5.527	$tonCO_2$/annum
S	123.6	$	zCO_2	14.5	$/ton$CO_2$
SFF	0.0139		ZCO_2 E.H	80.14	$/year
ASV	1.718	$	ZCO_2 new	72.4	$/year

Table 5.8. Comparison of the two methods.

Parameters	Electric heater method	New method
Defrost Energy Source	Electric heater	Condensing heat
Defrost efficiency	15.5%	100%
Temperature fluctuation	15°C	4.5°C
COP	1.94	2.23
Costs of the system	$563	$618
Annual power consumption	2763.7 kWh	2496.6 kWh
Annual cost of 1 kW of Q_E	$182.00	$147.10
CO_2 emissions/year	5.527 ton/year	4.993ton/year

5.5. ERROR ANALYSIS RESULTS

The accuracy of the devices used in the experiment is given in Table 5.9 and more details for these instruments can be found in Appendix A. Equation 4.40 was used to determine COP and η_{gen} errors, which were found to be 1.2% and 1.6%, respectively

Table 5.9. Accuracies of the instruments used for the measurement.

Instrument	Name	Range	Accuracy
Temperature	K-type Thermocouple	−40℃ to 375℃	±1.5
Pressure sensor	Testo 549i	−1 bar to 60 bar	±0.5%
Wattmeter	Kohler	0.1 A to 10 A	±1.0%
Charging scale	RES-100	0 kg to 100 kg	±0.5%

PART 6

CONCLUSION

6.1 CONCLUSION AND DISCUSSION

The main conclusions from this study are outlined below. This research sought to i) conduct a thorough review of the literature related to a number of defrosting methods, frost build-up, defrosting dynamics, and demands to defrost; ii) design, build and commission an experimental test facility capable of operating in the traditional manner (i.e., the electric heater method) and in the new method; iii) calculate the defrosting efficiency for both methods; and iv) to conduct an exergy, energy, economic, and environmental analysis (4E analysis) and compare the results between both methods. The cold storage rooms were designed to operate a conventional cold room where the defrosting process was conducted through the use of an electric heart. Since the new method uses a four-way valve and two evaporators, both of the systems were tested at the ambient temperature of 19.3℃ and at a cold temperature of −20℃ ± 2℃. In each method, the power consumption, pressure, and temperature were recorded and plotted on the log P-h diagram in order to identify the thermodynamic parameters and be used in the energy, economic, and exergy environmental analysis. The conclusions of this study can be summarized as follows:

1. The defrosting process of the new method could be conducted with the use of the heat from the liquid line refrigerant without adding further energy to the system. The increased sub-cooling leads to a 60-percent decrease in temperature fluctuation and an enhancement of system performance by 12%.
2. Uninterrupted refrigeration would accelerate the cooling process and decrease the time required to reach the required temperature.
3. The change of pressure when the four-way valve opens is smoother in comparison to reverse cycle and bypass methods.

4. The thermodynamic analysis showed that the heat gained by defrosting the evaporator would increase This heat load was due to the loss of heat from the defrosted evaporator.
5. Economic analyses for both methods showed that the new method lowered the annual cost of 1 kW of the cooling capacity (Q_E) from $182 to $147.10.
6. The enviro-economic analysis of the system for both methods showed that the new method decreased power consumption from 2,783.7 kWh to 2,496.6 kWh per year, annual CO_2 emissions mitigation per year (ϕ_{CO_2}) decreased from 5.527 tonCO_2 per year to 4.993 tonCO_2 per year.

The key points are expanded as follows:

The defrosting process of the new method was conducted with the use of the heat from the liquid line refrigerant without adding further energy into the system. The increase in sub-cooling in the liquid line due to heat absorbed from the defrosted evaporator would lead to a decrease in power consumption in the compressor and an increase in cooling capacity and COP. This leads to improving the refrigeration system efficiency in the new method by 12%, which is better than using the electric heater method in the same system. Since there is no further energy or time for defrosting, it becomes possible to use a short interval between the defrosting cycles to save the evaporator at high capacity and use evaporators with a small gap between fins. This increases the evaporator capacity for the same volume, thereby leading to a decrease in the evaporator cost. The cooling system was continuous because it does not stop defrosting. The temperature fluctuations occurring in the refrigerated compartment during the defrost process were about 14.5℃ in the Electric Heater Defrost Method. This rise in temperature is due to heat loss from the heater to the compartment. The temperature fluctuations are about 4.5℃ in the new defrosting method. A large amount of heat loss occurred in the electric heater method because, in the new method, the defrost heat occurs at the same place where frost is accumulated (in the pipe). However, in the electric heater, heat is generated in the heater and transferred to the fins rather than to the pipes with a large part of the heat transferring to the air. The defrosting efficiency is 15.5% in the electric heater method. The change of pressure when the four-way valve turns on is smoother in comparison to the reverse cycle and bypass methods in the literature. Moreover, the current rise when the reverse process

occurs between evaporators is lower than the initial current as seen in the power consumption diagram. The thermodynamic analysis shows that the heat gain from the melted evaporator increases the cooling load and is beneficial in increasing the subcooling in the liquid line, which leads to an improvement in system performance. The economic analysis for both methods showed that the new method decreased the annual cost of 1 kW of the cooling capacity (Q_E) by 20% (from \$182.00 to \$147.10), but the costs of the system increased by 10% (from \$563 to \$618). Although the initial installation cost of the new method is \$55 more than the electric heater method, the annual power consumption (APC) decreases by 11% (from 2763.7 kWh to 2469.6 kWh) and the annual electric cost (AEC) falls by 10% (from \$259.7 to \$234.6). This shows that the new method can recover its cost in a short time. The environmental analysis of the system for both methods showed that the new method decreased the annual CO_2 emission amount by 10.7% from (5.527 tonCO_2 per year to 4.993 tonCO_2 per year). Moreover, the new method appears to be more environmentally friendly than the electric heater method.

6.2 COMPARISONS WITH DATA IN THE LITERATURE

Many studies mention the development of demand defrost controls as an alternative for timed defrosting in order to avoid unneeded defrosting and to decrease the consumption of energy. In all of the previous studies on defrosting, the defrost process takes time and energy to melt the frost from the evaporator. Therefore, in this study, we endeavor to compare this study with some literature results.

In the paper "Study on the performance liquid refrigerant defrosting system" presented by M. Wang and R. Zang (2018), the method is enhanced by using the liquid refrigerant that leads the high-pressure in the receiver to defrost the evaporator. The system contains two evaporators, eight solenoid valves, and two check valves. During the defrosting process, the refrigeration cycle is continuous at half capacity with no additional consumption of energy. The findings of the study showed that the compressor power during the defrost process decreased by 60% from 2.0 kW to 0.8 kW. In this study, two evaporators and a four-way valve were used, and the refrigeration cycle was continuous at full capacity during the defrosting process

without any additional energy used for defrosting. The defrost process operated at the same time as the cooling process.

The change of pressure when the four-way valve turns on is smoother in comparison to the reverse cycle and bypass methods in a study presented by Huang, D., Li, Q., and Yuan, X. (2009). Comparisons are made between the hot-gas bypass defrosting and reverse-cycle defrosting methods on an air-to-water heat pump.

6.3 RECOMMENDATIONS FOR FUTURE WORK ON THIS TOPIC

The model that has been designed in this study is the first step in this new method for defrosting evaporators in refrigeration systems. In most facilities, defrost cycles are established by a time clock set. The defrost sequence has a timer clock that controls the time to initiate a defrost and determining the initiation of the defrost time is very important to keep the evaporator at high efficiency. However, the defrosting process should begin before the evaporator loses 10% of its capacity, as shown in Figure 2.4, to maintain airflow, capacity, and efficiency at a high level [7].

1. An automatic control system should be installed and set at the optimum duration for change in the four-way valve direction by adjusting the interval between defrosting the evaporators.
2. In order to improve the performance of this method, clips in front of the evaporators should be installed so that they close during the defrosting process and open during the cooling process to prevent the heat gains from the defrosted evaporator which raise the cooling load by 8%.
3. The tests should be run for longer periods and at various ambient temperatures because the defrosting process depends on the condensation temperature of the liquid refrigerant.
4. If the new method is used in the heat pump, it is more efficient because the heat loss in the defrosted evaporator will not be taken into account.

REFERENCES

1. Donnellan, W., "Investigation and Optimisation of Demand Defrost Strategies for Transport Refrigeration Systems", ***Dergi,*** Turkey, 45-55 (2007).

2. Subramaniam, P., and Wareing, P., "The stability and shelf life of food", ***Woodhead Publishing***, Germany, 23-31 (2016).

3. Bogdanovská, G., Stehlíková, B., and Kačur, J., "Analysis of Temperatures in the Cold Storage of Finished Products", ***Adv. Sci. Technol. Res. J***., 13 (3): 54-66 (2019).

4. Rodríguez-Rodríguez, D., Malak, D. A., Soukissian, T., and Sánchez-Espinosa, A., "Achieving Blue Growth through maritime spatial planning: Offshore wind energy optimization and biodiversity conservation in Spain", ***Mar. Policy***, 7(3): 8-14 (2016).

5. Sanner, B., "Ground source heat pumps—history, development, current status, and future prospects," ***12th IEA Heat Pump Conference***, Rotterdam, 1-14 (2017).

6. Pérez, L. C., "Novel defrost techniques on air source heat pumps Shoaib Azizi", ***Dergi,*** Turkey, 56-68 (2016).

7. Internet: Dudley, J., and Manager, R. S., "Commercial refrigeration temperature & defrost control and optimization", **https://pdf4pro.com/view/commercial-refrigeration-temperature-amp-defrost-22394f.html/** (2020).

8. Cai, J., "Control of Refrigeration Systems for Trade-off between Energy Consumption and Food Quality Loss", Aalborg University, Denmark, 67-78 (2007).

9. Knabben, F. T., and Melo, C., "An experimental study on the effect of a new defrosting strategy on the energy consumption of household refrigerator", ***Proc. 23rd ABCM Int. Congr. Mech. Eng***., Brazil, 12-19 (2015).

10. Dossat, R. J., and Horan, T. J., "Principles of Refrigeration", ***Prentice, Fifth Edit.,*** USA, 45-51 (2001).

11. Cho, H., Kim, Y., and Jang, I., "Performance of a showcase refrigeration system with multi-evaporator during on-off cycling and hot-gas bypass defrost", ***Energy***, 30(10): 1915-1930 (2005).

12. Alebrahim, A. M., and Sherif, S. A., "Electric defrosting analysis of a finned-tube evaporator coil using the enthalpy method", ***Proc. Inst. Mech. Eng. Part C J. Mech. Eng. Sci.***, USA, 34-45 (2002).

13. Ozyurt, B., Karatas, H., Inan, C., Egrican, N., and Hocaoglu, S., "Defrost efficiency in a no-frost-type household refrigerator/Discussion," ***Ashrae Trans.***, 10(8): 460 (2002).

14. Strong, A. P., "Hot gas defrost for industrial refrigeration", ***Heating Pip. air Cond.***, 60 (7): 71-83 (1988).

15. Mago, P. J., and Sherif, D. S. A., "Modeling the cooling process path of a dehumidifying coil under frosting conditions", ***J. Heat Transf.***, 124(6): 1182-1191 (2002).

16. Miller, W. A., "Laboratory examination and seasonal analysis of frosting and defrosting for an air-to-air heat pump", ***Ashrae Trans.***, 9(3): 1474-1489 (1987).

17. Peng, X., Xing, Z., and Shu, P., "Operating characteristics of an air-source heat pump under frosting/defrosting conditions", ***Proc. Inst. Mech. Eng. Part A J. Power Energy***, 217(6): 623-629 (2003).

18. Nawaz, K., Elatar, A. F., and Fricke, B. A., "A Critical Literature Review of Defrost Technologies for Heat Pumps and Refrigeration Systems", ***Oak Ridge National Laboratory,*** USA, 56-71 (2018).

19. Dong, J., Deng, S., Jiang, Y., Xia, L., and Yao, Y., "An experimental study on defrosting heat supplies and energy consumptions during a reverse cycle defrost operation for an air source heat pump," ***Appl. Therm. Eng.***, 3(7): 380-387 (2012).

20. Qu, M., Xia, L., Deng, S., and Jiang, Y., "An experimental investigation on reverse-cycle defrosting performance for an air source heat pump using an electronic expansion valve", ***Appl. Energy***, 9(7): 327-333 (2012).

21. Stoecker, W. F., "How frost formation on coils affects refrigeration systems", ***Refrigerating Engineering***, 65(2): 556-567(1957).

22. Niederer, D. H., "Frosting and defrosting effects on coil heat transfer", ***Ashrae Trans.***, 82(1): 467-473 (1976).

23. Stoecker, W. F., "Industrial refrigeration handbook", ***McGraw-Hill,*** New York,78-89 (1998).

24. Fisk, W., Archer, K., Raymond, C. and Hekmat, D., "Performance of residential air-to-air heat exchangers during operation with freezing and periodic defrosts", ***Ashrae Transactions,*** 91(1): 159-172. (1984).

25. Payne, V., and O'Neal, D. L., "Examination of alternate defrost strategies for an air-source heat pump: multi-stage defrost", ***in Winter Annual Meeting of the American Society of Mechanical Engineers,*** 2(8): 71–77 (1992).

26. Lee, T. H., Lee, K. S., and Kim, W. S., "The effects of frost formation in a flat plate finned-tube heat exchanger", ***International Refrigeration and Air Conditioning***, South Korea, 34-41 (1996).

27. Payne, W. V., and O'Neal, D. L., "The Effects of Outdoor Fan Airflow on the Frost/Defrost Performance of an Air-Source Heat Pump", ***Heat pump Refrig. Syst. Des. Anal. Appl.***, USA, 189-196 (1993).

28. Aljuwayhel, N. F., Reindl, D. T., Klein, S. A., and Nellis, G. F., "Experimental investigation of the performance of industrial evaporator coils operating under frosting conditions", ***Int. J. Refrig.***, 31(1): 98-106 (2008).

29. Özen, D. N., Altınışık, K., Dıncer, K., and Ateş, A., "Experimental Investigation and Numerical Modeling of Thermal Performance of Fin-Tube Evaporator Under Frosting Conditions", ***Isı Bilim. ve Tek. Derg.***, 34(2): 49-60 (2014).

30. De Aguiar, M. L., Gaspar, P. D., and Da Silva, P. D., "Frost measurement methods for demand defrost control systems: A review", ***Lect. Notes Eng. Comput. Sci.***, 2236: 671-677 (2018).

31. Da Silva, D. L., Hermes, C. J. L. L., and Melo, C., "Experimental study of frost accumulation on fan-supplied tube-fin evaporators", ***Appl. Therm. Eng.***, 31(7): 1013-1020 (2011).

32. Ye, H. Y., and Lee, K. S., "Performance prediction of a fin-and-tube heat exchanger considering air-flow reduction due to the frost accumulation", ***Int. J. Heat Mass Transf.***, 6(7): 225-233 (2013).

33. Moallem, E., Hong, T., Cremaschi, L., and Fisher, D. E., "Experimental investigation of an adverse effect of frost formation on microchannel evaporators, part 1: Effect of fin geometry and environmental effects", ***Int. J. Refrig.***, 36(6): 1762-1775 (2013).

34. Wu, X., Chu, F., Ma, Q., and Zhu, B., "Frost formation and frost meltwater drainage characteristics on aluminum surfaces with grooved structures", ***Appl. Therm. Eng.***, 11(8): 448-454 (2017).

35. Sommers, A. D., Truster, N. L., Napora, A. C., Riechman, A. C., and Caraballo, E. J., "Densification of frost on hydrophilic and hydrophobic substrates - Examining the effect of surface wettability", ***Exp. Therm. Fluid Sci.***, 7(5): 25-34 (2016).

36. Long, Z., Jiankai, D., Yiqiang, J., and Yang, Y., "A novel defrosting method using heat energy dissipated by the compressor of an air source heat pump", ***Appl. Energy***, 13(3): 101-111 (2014).

37. Yoon, Y., Jeong, H., and Lee, K. S., "Adaptive defrost methods for improving defrosting efficiency of a household refrigerator", ***Energy Convers. Manag***., 15(7): 511-516 (2018).

38. Liu, Z., Gao, W., Lang, H., and Chi, Y., "Experimental study on a new type of defrosting system using outdoor air for frost-free household refrigerators", ***Appl. Therm. Eng***., 13(4): 256-265 (2018).

39. Stoecker, W. G. F. , Lux Jr, J. J., and Kooy, R. J., "Energy considerations in hot-gas defrosting of industrial refrigeration coils", ***Ashrae Trans***., 8(9): 549-573 (1983).

40. Kerschbaumer, H. G., "Analysis of the influence of frost formation on evaporators and of the defrost cycles on performance and power consumption of refrigeration systems", **in *Proceedings of the 13th International Congress of Refrigeration***, USA, 1-12 (1971).

41. Cole, R. A., "Refrigeration loads in a freezer due to hot gas defrost and their associated costs", ***Ashrae Trans.***, 9(5): 609-890 (1989).

42. Al-Mutawa, N. K., Sherif, S. A., and Mathur, G. D., "Determination of coil defrosting loads: Part III--testing procedures and data reduction", ***Ashrae Trans.***, 10(4): 303 (1998).

43. Kim, M. H., Kim, H., Kim, D. R., and Lee, K. S., "A novel louvered fin design to enhance thermal and drainage performances during periodic frosting/defrosting conditions", ***Energy Convers. Manag***., 1(10): 494-500 (2016).

44. Modarres, F. G., Rasti, M., Joybari, M. M., Nasrabadi, M. R. F., and Nematollahi, O., "Experimental investigation of energy consumption and environmental impact of adaptive defrost in domestic refrigerators", ***Meas. J. Int. Meas. Confed***., 9(2): 391-399 (2016).

45. Zhao, R., Huang, D., Zhang, Z., and Leng, Y., "Effect of defrosting heat leakage on freezer temperature rise during periodical defrost cycles in a frost-free refrigerator-freezer with an electric defrost heater", ***Sci. Technol. Built Environ***., 23(1): 211-217 (2017).

46. Wang, M., and Zang, R., "Study on the performance liquid refrigerant defrosting system", ***Therm. Sci. Eng. Prog***., 8(2): 105-108 (2018).

47. Zheng, X., Shi, R., You, S., Han, Y., and Shi, K., "Experimental study of defrosting control method based on image processing technology for air source heat pumps", ***Sustain. Cities Soc***., 5(2): 101667 (2019).

48. Zhao, R., Huang, D., Peng, X., and Qiao, L., "Comprehensive measures to enhance electric heater defrosting (EHD) performance for household frost-free refrigerators", ***Int. J. Refrig***., 1(11): 1-8 (2020).

49. Malik, A. N., Khan, S. A., and Lazoglu, I., “A novel hybrid frost detection and defrosting system for domestic refrigerators”, ***Int. J. Refrig***., 11(7): 256-268 (2020).

50. Parker, D. S., Huang, Y. J., Konopacki, S. J., & Gartland, L. M., "Measured and simulated performance of reflective roofing systems in residential buildings", ***Ashrae Transactions,*** 10(4): 963 (1998).

51. Ay, M., Midilli, A., and Dincer, I., “Thermodynamic modeling of a proton exchange membrane fuel cell”, ***Int. J. Exergy***, 3 (1): 16-44 (2006).

52. Kanoglu, M., Dincer, I., and Rosen, M. A., “Exergetic performance investigation of a turbocharged stationary diesel engine”, ***Int. J. Exergy***, 5(2): 193-203 (2008).

53. Chandrasekharan, M., “Exergy analysis of vapor compression refrigeration system using R12 and R134a as refrigerants”, ***Int. J. Students’ Res. Technol. Manag.***, 2(4): 134-139 (2014).

54. Özgür, A. E., Kabul, A., and Kizilkan, Ö., “Exergy analysis of refrigeration systems using an alternative refrigerant (HFO-1234yF) to R-134a”, ***Int. J. Low-Carbon Technol.***, 9(1): 56-62 (2014).

55. Maiorino, A., Aprea, C., Duca, M. G. D., Llopis, R., Sánchez, D., and Cabello, R., “R-152a as an alternative refrigerant to R-134a in domestic refrigerators: An experimental analysis”, ***Int. J. Refrig***., 9(6): 106-116 (2018).

56. Akpinar, E. K., and Hepbasli, A., “A comparative study on exergetic assessment of two ground-source (geothermal) heat pump systems for residential applications”, ***Build. Environ***., 42(5): 2004-2013 (2007).

57. Kotas, T. J., “The exergy method of thermal plant analysis”, ***Elsevier,*** Germany, 34-39 (2013).

58. Yumrutaş, R., Kunduz, M., and Kanoğlu, M., “Exergy analysis of vapor compression refrigeration systems”, ***Exergy, An Int. J***., 2(4): 266-272 (2002).

59. Bansal, P., Fothergill, D., and Fernandes, R., “Thermal analysis of the defrost cycle in a domestic freezer”, ***Int. J. Refrig***., 33(3): 589-599 (2010).

60. Gin, B., Farid, M. M., and Bansal, P. K., “Effect of door opening and defrost cycle on a freezer with phase change panels”, ***Energy Convers. Manag***., 51(12): 2698-2706 (2010).

61. Deniz, E., and Çınar, S., “Energy, exergy, economic and environmental (4E) analysis of a solar desalination system with humidification-dehumidification”, ***Energy Convers. Manag***., 12(6): 12-19 (2016).

62. Kianifar, A., Heris, S. Z., and Mahian, O., “Exergy and economic analysis of a pyramid-shaped solar water purification system: active and passive cases”, ***Energy***, 38(1): 31-36 (2012).

63. Tiwari, G. N., Yadav, J. K., Singh, D. B., Al-Helal, I. M., and Abdel-Ghany, A. M., “Exergoeconomic and enviroeconomic analyses of partially covered photovoltaic flat plate collector active solar distillation system”, ***Desalination***, 36(7): 186-196 (2015).

64. M. O. A. Abdulla, E. Deniz, M. Karagöz, and G. Gürüf, “An experimental study on a novel defrosting method for cold room,” ***Appl. Therm. Eng***., vol. 188, no. January, p. 116573, 2021, doi: 10.1016/j.applthermaleng.2021.116573.

APPENDIX A.

DATA ACQUISITION SYSTEMS DETAILS

PRESSURE PROBE MEASUREMENT

Figure Appendix 1. Pressure sensor Testo 549i.

.

Table Appendix 1. The general data for pressure sensor Testo 549i.

Property	**Value**
Sensor Type	Pressure
Measuring Range	−1 bar to 60 bar
Accuracy	0.5% of the final value
Resolution	(0.1 psi) 0.0067 bar
Connection	7/16" – UNF
Overload Rel.	65 Bar
Storage Temperature	−20 to 60°C
Operating Temperature	−20 to 50°C
Dimensions	12.5 cm × 3.3 cm × 3.0 cm
Measuring Units	bar, psi, MPa, kPa
Measurable Media	CFC, HFC, HCFC, N, H_2O, CO_2

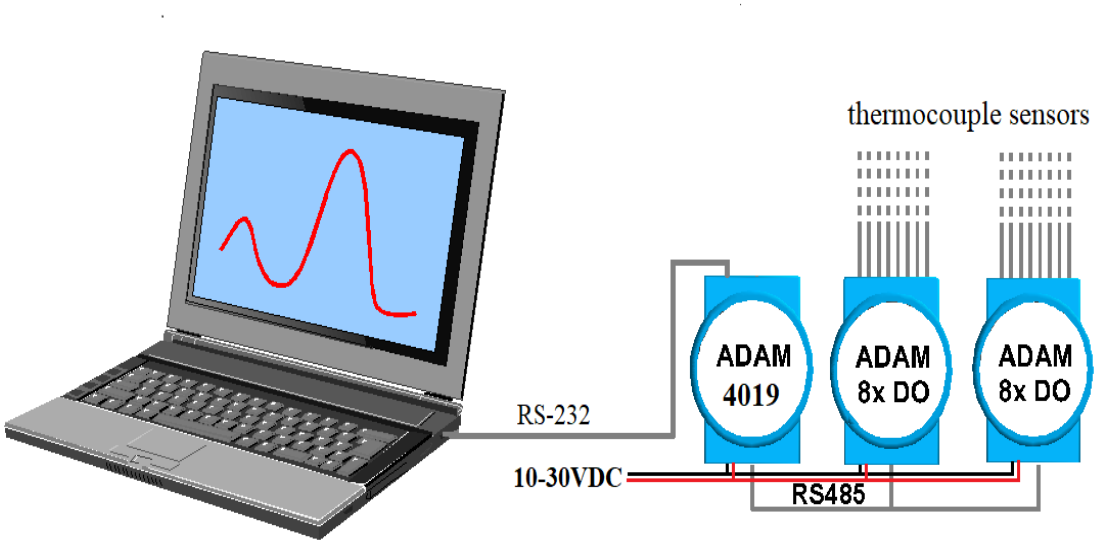

Figure Appendix 2. Basic hook-up of ADAM module to host switches.

Table Appendix 2. Technical specification of ADAM with thermocouple input modules.

Channels	8	
Input Range	+/−20 mA 4-20 mA	
Calibration Accuracy	+/−0.1% or better	
Power Consumption	0.8 W @ 24 V_{DC}	
Sampling Rate	10 samples/sec (total)	
Range and Accuracy for Thermocouple		
Input Range	**Typical Accuracy**	**Maximum Error**
K thermocouple 0°C to 1000°C	0.5°C	0.75°C
T thermocouple −100°C to 400°C	0.5°C	0.75°C
R thermocouple 500°C to 1750°C	0.6°C	1.5°C
B thermocouple 500°C to 1800°C	1.2°C	2.0°C

Figure Appendix 3. Digital programmable electronic charging scale RES-100.

Table Appendix 3. Specifications of electronic charging scale RES-100.

Property	Value
Capacity	100 kg/220; bs
Accuracy	+/−0.5% of reading
Resolution	+/−0.2 oz/0.01 lbs/5 g
Platform Size	23 cm × 23 cm
Weight	3.6 kg
Power	2 pcs 5 AA battery included (60 hours)
Operating Temperature	0°C to 50°C
Storage Temperature Range	−20 to 70°C
Auto-off	15 min
Has memory function	Yes

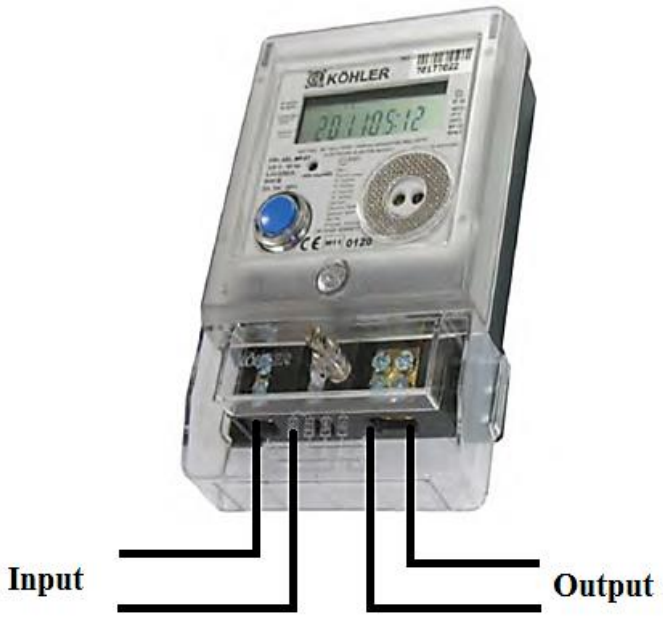

Figure Appendix 4. Köhler model AEL.MF.07 ampere active single-phase counter.

Table Appendix 4. Köhler powermeter specification.

Model Name	**AEL.MF.07_B**
Reference Voltage:	230 V
Frequency:	50 Hz
Take-off Current:	20 mA
Max/Min Current:	0.25 A/90 A
Accuracy Class:	±1.0%
Relative Humidity Rate:	95%
Operating Temperature:	−40°C to +80°C
Energy Records:	12-Month Index and Demand Information

RESUME

Mahade Omran Ali ABDULLA was graduated primary, elementary, and high school in his city in LIBYA, after that, he started an undergraduate program at the Higher Institute of Refrigeration and Air-condition in SOKNA on1998, he attended Master of Mechanical Engineering (M.Sc.) from The Technical University of Kosice Slovakia 2004. Then in 2016, he started at Karabük University Mechanical Engineering to complete his Ph. D. education.